

EChEMA: ElectroChemical Sensors for Heavy Metal Analysis in Point of Care Applications

BY

ELENA BOSELLI

B.S., Politecnico di Milano, Milan, Italy, July 2016

THESIS

Submitted as partial fulfillment of the requirements
for the degree of Master of Science in Bioengineering
in the Graduate College
of the University of Illinois at Chicago, 2018

Chicago, Illinois

Defense Committee:

Ian Papautsky, Chair and Advisor

David Eddington

Marco Carminati, Politecnico di Milano

This thesis is dedicated to my parents, Irene and Ambrogio and to my sister Francesca, the white “lúdesan” gazelle . Without them I wouldn’t probably be even arrived at the first year of the university.

ACKNOWLEDGMENTS

First of all I'd like to thank my advisor, Dr. Ian Papautsky, for his constant support during these months. I really appreciate his sincere help to cope with all the difficulties I encountered.

In this regard I cannot forget to express my gratitude to Dr. Thushani Siriwardhane, who opened me the doors of the magic and tricky world of electrochemistry. I'd like also to thank all of the committee members, Dr. David Eddington and my Italian advisor, Dr. Marco Carminati, for their availability, especially in the last few weeks. A special remark goes to Dr. William Heineman, for his bright suggestions in the darkest period of my work, when nothing seemed to go in the right course and to Ms. Lynn Thomas, for her assistance on the formal side of the project; one of the most common sentences in our apartments during all of these months was: "*ask Lynn, she'll find a solution*".

I cannot forget to mention my lab mates, Dr. Jian Zhou and Dr. Hua Gao for giving me an insight in the Chinese culture. The other two guys, Nebu and Prithvi have been simply essential; without them I would have given up several days before completing the project; they raised in me the passion for research and for my work during our lab afternoons, in between an experiment and a cup of Lavazza coffee. A particular thank goes to all the italian-chicagoan students, for our lunches and dinners together.

A thank goes to my flatmates: to Bea, for sharing with me some of her cooking secrets; to Leo, besides the open cabinets and squashes in the sink; to Marti, for our travels on the blue line at late night among the "disagini friends"; to Greta, for her laughs and her delicious risotti that helped me to overcome all of the obstacles. There are no words to thank Vicky, for our dances on the rhythm of *mi gente* and our lesson reviews at the SEO and MZampi, the greatest showman, for the timewarp, Maria and Geronimo; they always showed me the light at the end of the tunnel. I am fully aware that it is not easy to live with me and I really appreciate their patience.

I cannot forget the part of me on the other side of the atlantic ocean and I have to thank all of my friends and relatives, but especially Agnese, Sere, Deni, Martola, Caro and Francis; the memories of our funny moments together gave me the strength in the grey and freezy days here in Chicago.

There are no words to thank my parents, Irene and Ambrogio.

The last remark goes to the other half of me, my squash Franz; she's simply my person, either when close together or when far away.

All of you made my chicagoan dream come true.

EB

TABLE OF CONTENTS

<u>CHAPTER</u>		<u>PAGE</u>
1.	INTRODUCTION.....	1
1.1	Lead (Pb) toxicity.....	3
1.2	Manganese (Mn) toxicity.....	4
2.	TECHNIQUES FOR HEAVY METAL DETECTION AT TRACE LEVEL...	6
2.1	AAS : Atomic Absorption Spectroscopy.....	6
2.2	ICP-MS : Inductively Coupled Plasma Spectrometry	7
2.3	Electrochemical techniques.....	8
2.4	Classification.....	12
2.5	Potentiostatic techniques for trace element detection.....	13
2.6	Stripping voltammetry: the importance of preconcentration.....	14
2.7	Square Wave voltammetry: rejection of the background current.....	15
2.8	SWASV vs SWCSV.....	19
3.	MATERIALS AND METHODS.....	21
3.1	Reagents.....	21
3.2	Sensors.....	22
3.3.	Whole blood digestion.....	26
3.4	Standard Addition.....	28
3.5	Software.....	29
4.	RESULTS AND DISCUSSION.....	30
4.1	Lead detection on Au electrodes.....	30
4.2	Optimization of the SWASV parameters.....	31
4.3	Calibration.....	38
4.4	Human Blood.....	40
4.5	Manganese detection on Pt electrodes.....	44
4.6	Optimization of the SWCSV parameters.....	46
4.7	Calibration.....	50
4.8	Human blood.....	51
5.	CONCLUSIONS AND WORK IN PROGRESS.....	52

LIST OF TABLES

<u>TABLE</u>		<u>PAGE</u>
I	SQUARE WAVE PARAMETERS.....	17
II	CHARACTERISTICS OF SWASV VS SWCSV.....	19
III	SPECIFICATIONS OF THE APPLIED SENSORS ED-SE1.....	23
IV	DIGESTION PROCESS: PROTOCOL COMPARISON.....	27
V	OPTIMIZED PARAMETERS FOR SWASV OF PB IN STANDARD SOLUTIONS, ELECTROLYTE: AB pH5.2.....	37
VI	STANDARD ADDITION SPECIFICATIONS.....	40
VII	OPTIMIZED PARAMETERS FOR SWCSV OF Mn IN STANDARD SOLUTIONS, ELECTROLYTE: BB pH8.9.....	50

LIST OF FIGURES

<u>FIGURE</u>	<u>PAGE</u>
1. Sensor compared to the dimension of one cent coin.....	5
2. General scheme of electrochemical detection.....	9
3. Simplified electrical equivalent of a three electrode setup.....	10
4. Classification tree of electrochemical techniques.....	12
5. Basic schematic of a potentiostat.....	13
6. Example of excitation waveform for SWCSV.....	15
7. Example of excitation waveform with square wave parameters.....	17
8. Comparison ASV vs CSV.....	20
9. Inset on the active surface of the sensor.....	22
10. Overview of the setup during an experiment.....	24
11. Chronopotentiogram during chloridization of the reference electrode.....	25
12. Pt and Au electrodes after each phase of electroplating.....	26
13. Comparison digested human blood before and after pH adjusting.....	28
14. Cyclic Voltammetry on Au electrodes.....	31
15. Voltammograms of Pb in at different deposition potentials.....	33
16. Anodic current peaks versus deposition time.....	34
17. Current peaks and FWHM versus square wave amplitude.....	35
18. Linear model current peaks – square wave period.....	36
19. Current peaks and FWHM vs square wave period.....	37
20. Example of a series of voltammograms at different Pb concentrations.....	38
21. Linear regression model for the calibration curve of Au electrodes.....	39

LIST OF FIGURES (continued)

<u>FIGURE</u>	<u>PAGE</u>
22. Linear regression model human blood samples: first trial.....	41
23. Voltammograms obtained from analysis of human blood.....	42
24. Linear regression model human blood samples: second trial.....	42
25. Cyclic voltammetry Pt electrodes: electrolyte comparison.....	44
26. Cyclic voltammetry Pt electrodes: acetate buffer and 20ppm Mn.....	45
27. Cyclic voltammetry Pt electrodes borate buffer.....	46
28. Optimization deposition time.....	47
29. Optimization square wave period.....	48
30. Optimization square wave amplitude.....	49
31. SWCSV 5ppb Mn in borate buffer pH 8.9.....	51

LIST OF SYMBOLS

POC	=	point-of-care
AAS	=	atomic absorption spectroscopy
ICP-MS	=	inductively coupled plasma mass spectrometry
CNS	=	central nervous system
WE	=	working electrode
CE	=	counter electrode
RE	=	reference electrode
SWASV	=	square wave anodic stripping voltammetry
SWCSV	=	square wave cathodic stripping voltammetry
ppb	=	parts per billion
ppm	=	parts per million
CDC	=	center for disease and control and prevention
LOC	=	lab-on-a-chip
LOD	=	limit of detection
Pb	=	lead
Mn	=	manganese
Au	=	gold
Pt	=	platinum

SUMMARY

Healthcare monitoring still lacks of point-of-care (POC) devices for heavy metal detection in human blood. Gold standard techniques currently employed – (AAS) atomic absorption spectroscopy and (ICP-MS) inductively coupled plasma mass spectrometry - require voluminous and expensive equipments, specialized personnel and large sample volumes to perform the analysis. These characteristics make them unfeasible for on-the-field applications^[1,2]. On the other side, electrochemical detection of heavy metals can be pursued with cost effective, disposable sensors and little amount of volumes. Lead (Pb) and Manganese (Mn) levels are worth to be monitored as target toxicant metals. Reasons for this assumption include their increasing presence in the environment associated to human activities and their severe impairment on the central nervous system (CNS) even at low exposure levels. Commercially available electrochemical sensors featuring gold (Au) working electrodes (WE) are applied for quantitative identification of lead (Pb) via square wave anodic stripping voltammetry (SWASV) , whereas the same devices with platinum (Pt) electrodes are analyzed for manganese evaluation through square wave cathodic stripping voltammetry (SWCSV). Despite all the efforts made by several research groups in environmental samples, little has yet been done on real human blood. Successful preliminary tests on human blood samples are achieved for lead determination and the right path for manganese has been traced. The ease of fabrication through well developed techniques and cost effectiveness of the sensors and the ability of handling small amount of volumes (droplets of 10 μ L) for each measurement make this approach a viable way for effective on-the-field application. In the next future its integration with microfluidic devices for sample preparation will bring to reality the dream for portable '*metallometers*'.

CHAPTER 1

INTRODUCTION

Heavy metal detection in biological fluid still lacks of small, cost effective devices. The ultimate goal of this research is the development of easy-to-use, low cost and small devices for point-of-care detection of trace metal levels in human blood. Heavy metals can be defined as metallic elements with a density at least 5x that of water ($\rho_{H_2O} = 1 \text{ g/cm}^3$)^[7]; considering the assumption that toxicity is strictly related to heaviness, it emerges that these elements can be health-threatening even at trace level, at concentrations in the part per billion (*ppb*, 10^{-6}) rather than part per million (*ppm*, 10^{-3}) range. Although the mechanisms of heavy metals intake on human health are unique for each compound and yet not fully understood, it is demonstrated that their systemic impairment can affect almost every cellular organelle from the cellular membrane to the nuclei and different enzymes involved in damage repair, metabolism and detoxification. Reactive Oxygen Species (ROS) are believed to play a fundamental role in mediating metal induced cell injuries^[6] that include the interactions with DNA and nuclear proteins, leading to cell changes, carcinogenesis and ultimately apoptosis. This study focuses on two particular metals: Lead (*Pb*, density $\rho_{Pb} = 11.34 \text{ g/cm}^3$) and Manganese (*Mn*, density $\rho_{Mn} = 7.43 \text{ g/cm}^3$).

The relevance of Pb detection even at low exposure levels is related to its widespread presence in everyday life. Lead sources common everywhere comprise paint, products made of plastic, vinyl and food, contaminated with lead during growth on soil, production, packaging or storage^[4].

On the other side, the interest in Mn detection arises from the subtle border between its importance as a key element in some biological functions and its toxicity related to neurodegenerative diseases and mental impairments in children even at reduced levels of exposure^[8].

The importance of this study can be further enhanced considering that their environmental levels have exponentially risen due to their release from several human activities, including industrial

processes, agriculture and technological fabrication^[3]. The established relationship between neurodegenerative diseases and exposure to heavy metals pushed forward research studies whose primary aim is the identification of the proper strategies for heavy metal determination^[9].

In spite of their abilities of multi-element analysis and very small limits of detection, both of the two actual gold standard techniques - AAS and ICP-MS - suffer from the impossibility of point of care adaptability^[20]. They require long analytical times, bulky instruments available only in analytical laboratories and manipulation of the sample by specialized personnel. Electrochemical techniques offer the possibility to overcome all of these issues, while achieving detection limits compatible with heavy metal levels in biological and environmental samples^[20,9]. Several sensors have been proposed to achieve heavy metal detection^[1,2,10,37], but they all require complicated fabrication processes that inevitably increase their cost of fabrication and make them suitable for academic purposes but impractical for real applications. In contrast, sensors based on noble metals electrodes, such as gold (Au) and platinum (Pt) are currently easily available on the market and performances fully compatible with heavy metal detection in biological fluids are demonstrated in this study. Cost effectiveness, ease of integration with other components and market availability are three fundamental features for a widespread diffusion of disposable diagnostic devices.

Moreover, considering Lead (*Pb*) and Manganese (*Mn*) toxicity in humans, as summarized in the following chapters, it is not difficult to imagine how much will be useful one day to develop portable E-CHeMA sensors or '*metallometers*' ready for heavy metal analysis at point-of-care level.

1.1. Lead (*Pb*) toxicity

Lead (Pb) is a highly toxic heavy metal whose natural presence in the environment is consistently increased by human activities. Despite US ban of lead based paints in housing in 1978 and as a gasoline additive, Lead exposure for humans still remains a major health problem due to its strong absorption into the soil and its slow deterioration. In humans three routes of exposure are mainly identified: 1) ingestion from contaminated food or drinking water, 2) inhalation from lead dust or fumes in industrial contexts, 3) dermal contact. In 2012 the CDC (Center for Disease Control and Prevention) fixed the value for elevated blood lead level in children at $5\mu\text{g/dL}$ (50ppb), with evidence that neurotoxic effects of lead exposure in workers are present at blood levels $\leq 18\mu\text{g/dL}$ (180ppb).

As a divalent cation (Pb^{2+}), lead binds to proteins sulphhydryl ($S - H$) groups with a subsequent distortion of their structure and functionality^[6]. It is capable of reaching almost every organ or system in human body but its main impairments affect the CNS (Central Nervous System), as a consequence of its ability to overcome the Blood Brain Barrier. Moreover, its neurotoxicity is found to be determinant for neurologic disfunctions in children such as lack of muscular coordination, intellectual and behavioral deficits^[6].

Blood has been recognized as the primary biomarker for the assessment of lead exposure. It is important to underline that Blood Lead levels (BPb) are capable of reflecting both recent and past exposure as a result of reabsorption into blood from bones^[11]; whole blood measurements must be considered since Pb mainly binds to proteins and erythrocyte and plasma Pb can be assumed to be the most relevant in terms of its toxicity as the compartment capable of more rapid exchange of Pb throughout the body^[12]. It turns out that constant monitoring of whole blood lead levels seems to be mandatory for a dual purpose: the first one is the assessment of long term exposure and the second one is early detection of high Pb levels, especially in work environments at high risk (mining, batteries, metal recycling industries) and in highly sensible subjects (children, pregnant women).

1.2. Manganese (*Mn*) toxicity

Mn is an element known to be essential in several enzymatic reactions including growth of neuronal and glial cells as well as synthesis and development of neurotransmitters^[16]. Moreover, it is involved in metabolic processes of fat and carbohydrates and in bone formation as a cofactor for calcium absorption^[9]. The thin border between Mn physiological impact and its toxicity makes this heavy metal monitoring in humans particularly important. Mn is the fourth most used metal in the world after iron, aluminum and copper. Mn exposure occurs primarily via inhalation^[13]; its chemical properties lead to its usage in the production of high resistant steel, glass, ceramics, weldings, adhesives, paints and gasoline, with a potential vulnerability for large part of the population. Mn has been addressed as an irritant of the respiratory tract and a cause for lung inflammations and decreased functionality^[13], although the most important impairment caused by Mn even at low levels are represented by neurodegenerative diseases, with symptoms often compared to the Parkinson's ones and associated with disfunctions in the basal ganglia system^[15]. The reversibility of this condition at the first stages makes an early detection of dangerous levels of Mn extremely important.

Monitoring of these threatening substances has been assessed as a public health priority by many international agencies including the European Union, the Joint Food and Agricultural Organization (FAO), the World Health Organisation (WHO) and the Centre for Disease Control (CDC), pushing forward the need for easy to use, low cost and small-sized sensors for on the field detection, as occurred for glucose levels checking with the modern and portable glucometers. Several steps are still necessary for a complete miniaturization of all the components involved in the heavy metal detection process, but as *Figure 1* exemplifies the right path for lab-on-a-chip (LOC) platforms is traced.

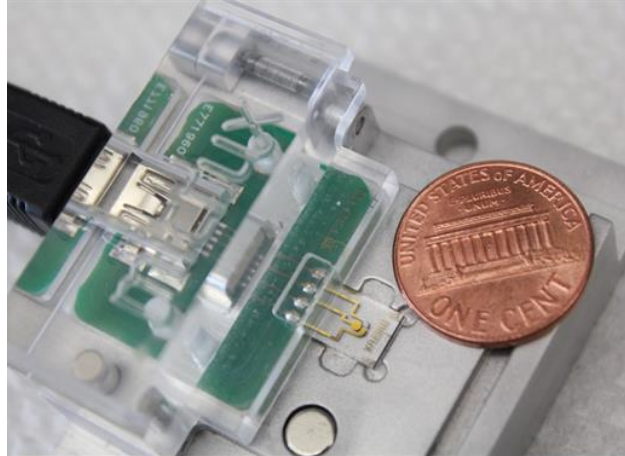


Figure 1-Dimensions of the miniaturized gold-based sensor for heavy metal detection used in this work compared to a one cent coin - sensor model ED-SE1 from Micrux Technologies

CHAPTER 2

TECHNIQUES FOR HEAVY METAL DETECTION AT TRACE LEVELS

2.1. AAS : Atomic Absorption Spectroscopy

One of the most used method for metallic detection in different sample matrices is represented by Atomic Absorption Spectroscopy. It allows quantification of a wide variety of species both at trace levels and at higher concentrations. This method measures the amount of energy (in the form of a wavelength change) absorbed by the excited sample. The analysis of a sample is based on the unique electron configuration that each atom presents in its outer shell and therefore only absorbs energy at a specific wavelength, related to the energy difference between its electronic levels. The quantification of the amount of the target substance is then derived from the intensity of the absorption spectrum on the basis of the Beer-Lambert's law:

$$A = \log_{10}\left(\frac{I_0}{I}\right) = \varepsilon(\lambda)Lc \quad (2.1)$$

Where A is the measured absorbance, I_0 is the intensity of light initially provided to the sample, I is the light intensity after passing through the sample – or the light intensity transmitted by the sample, $\varepsilon(\lambda)[M^{-1}cm^{-1}]$ is the wavelength dependent molar absorptivity coefficient, $L [cm]$ is the path traveled by the light through the sample and $c[M]$ is the concentration of the analyte in the evaluated sample.

AAS involves different steps that can be summarized in the following ones: 1)Atomization of the sample either in a graphite or in a flame furnace, 2)Irradiation of the treated sample either with UV or visible light sources, according to the specific target metal to be detected, 3) Measurement of the wavelength transmitted by the sample and comparison with the excitation wavelength originally passed through the sample.

Concentration of the analyte is then determined on the basis of calibration curves obtained from standards at known concentrations.

A number of specialized instruments is required to carry out this analysis and make it unfeasible for on the field or point of care (POC) applications.

2.2. ICP-MS: Inductively Coupled Plasma-Mass Spectrometry

Nowadays referred to as the most common technique employed in analytical laboratories for trace metal level determination. Its advantages encompass ultra low *LOD* in the part per trillion (ppt) range, simultaneous multielemental analysis and isotopic capabilities.

ICP-MS combines an ICP source at high temperature with a mass spectrometer for detection purposes. The inductively coupled plasma (ICP) source converts the atom of the elements in the sample into ions. These particles are then directed into the mass spectrometer by means of the interface region and focused in the system through a series of electrostatic lenses.

The heart of the ICP-MS is represented by the mass separation device, kept at high vacuum (*Pressure*~ 10^{-6} *Torr*). This component filters the generated ions on the basis of their ratio mass-to-charge. The final step after the splitting of the different ions is their conversion into a detectable electrical signal. The most common design for ions detection is a series of metal dynodes along the length of the instrument^[17].

It is evident that also this method turns out to be impractical for point of care detection and widespread use and provides incompatibility with a constant home-monitoring of heavy metal levels in humans.

As highlighted in the previous paragraphs the gold standard techniques applied for trace metal detection all suffer from the dependency on specific, bulky and costly equipment that prevent their

transition from analytical laboratories to home-take care. Thus, the only practicable way appears to be electrochemical detection.

2.3. Electrochemical techniques

Electrochemistry can be defined as the crossroad between electrical and chemical effects. It is a scientific field and an engineering tool that comprises several phenomena and technologies with a direct application in different devices ranging from common batteries to industrial fuel cells. The dual principle on which the basis of electrochemistry are built relies in the chemical changes produced by the passage of an electric current and the energy production generated by chemical reactions^[11].

Electrochemical analysis are concerned with the processes that develop at the interface between different chemical phases in a system referred to as an electrochemical cell. In the case of trace element detection the main actor is represented by the boundary between an *electrode* (i.e. an electronic conductor) and an *electrolyte* (i.e.a conductor where ions are the charge carriers). The electrolyte contains the heavy metal ions dissolved in a supporting media. Small electrodes can be exploited to pass a current to the liquid sample and generate a detectable electrical signal representative of the electrochemical reactions that took place at the interface due to the presence of the target metal ions.

These are active methods, since they require the presence of a power supply to provide the proper excitatory signal and consequently measure the response function given by the analyte under test; the general workflow for any electrochemical analysis is represented in *Figure 2*.

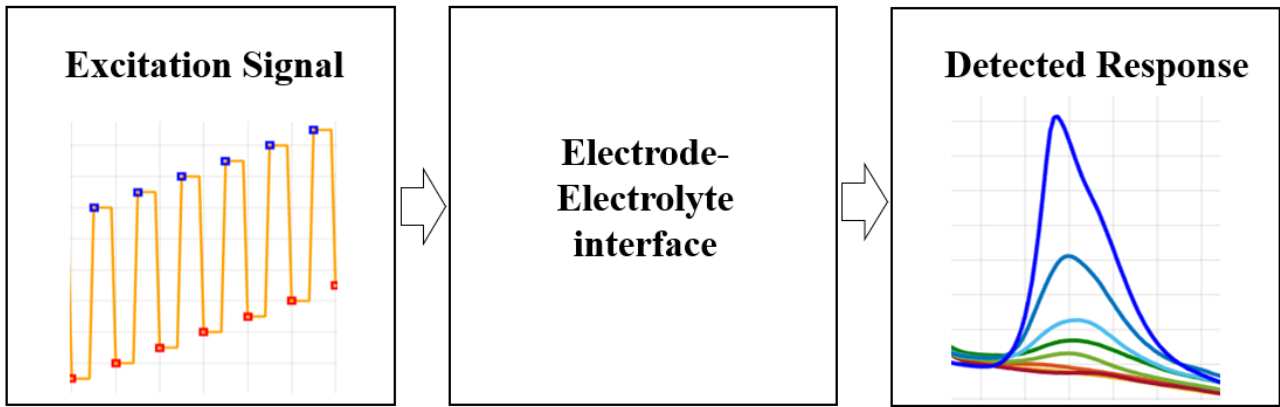


Figure 2-General scheme of electrochemical analysis. In this example the detected response is represented by a current vs potential curve, showing detectable peaks at different target concentrations.

The techniques involved in this study implement a three electrode setup that consists of a Reference Electrode(RE), a Counter Electrode(CE) and a Working Electrode(WE) . The basic configuration of the device needed to perform this kind of detection will be given in the following paragraph. When a biased solid electrode is in contact with an electrolyte three different phenomena may occur:

1. Potential drop at the interface due to the resistance of the solution R_{sol} (Built-in Potential)
2. Rearrangement of charges at the interface that induce the creation of a layer of ions very close to the solid conductor with opposite charges and is namely known as the double layer capacitance C_{dl}
3. Charge transfer between the ions of electroactive species in solution and the electrons in the solid conductor. This last process gives rise to the Faradaic current that is the relevant signal indicative of the concentration of the target analyte.

A simplified electrical equivalent of the system can be defined as a network of impedances and it is shown in *Figure 3*.

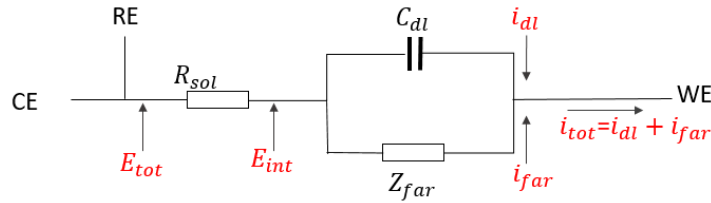


Figure 3-Electrical equivalent of a three electrode electrochemical cell–WE=WorkingElectrode, RE=ReferenceEllectrode ,CE=CounterElectrode, E_{tot} =controllable potential, E_{int} =effective potential seen at the electrode-electrolyte interface, R_{sol} =resistance of the solution, C_{dl} =double layer capacitance, Z_{far} =faradaic impedance, i_{tot} =effective current measured at the working electrode, i_{far} =current generated by the faradaic electron transfer between the electrolyte and the electrode, i_{dl} =current generated by the presence of the double layer capacitance.

Z_{far} is the faradaic impedance that represents the electron transfer at the working electrode and depends upon the kinetic at which this relevant phenomena occurs. The double layer capacitance C_{dl} and the faradaic process that generates the current i_{Far} occur at the interface, provide a parallel path for the electron delivery and are in series with the solution resistance R_{sol} ^[13]; given that, the total current i_{tot} that will flow through the working electrode will be the sum of the two components i_{Far} and i_{dl} . The interesting signal that relates to the presence and cincentration of the target is only the faradaic component i_{Far} and one of the advantages of the chosen technique of square wave voltammetry with respect to simple linear methods lies in the rejection of i_{dl} .

At this point it is substantial to underline the relevance of the reference electrode in a three electrode system with respect to a simple two electrode configuration-without RE- as a way to minimize the effect of the ohmic voltage drop that happens due to the presence of the solution resistance R_{sol} . As depicted in *Figure 3*, the controllable parameter is the overall potential E_{tot} , whereas the effective potential seen by the electrolyte-electrode interface E_{int} is somewhat different as a consequence of R_{sol} that represents a resistive path in series with the interface and leads to a potential difference across itself

$$E_{sol} = R_{sol} * i \quad (2.2).$$

$$E_{tot} = E_{sol} + E_{int} \quad (2.3)$$

From Equation (2.2) it is clear that E_{sol} depends upon the current signal and therefore cannot be precisely governed; the result is a distortion of the excitation signal seen by the interface for voltammetric techniques and an inaccuracy in the potential response signal for amperometric techniques^[12]. The most common approach to minimize this effect is to design the reference electrode (RE) as close as possible to the working one (WE). As pointed out in the previous sentences, the material of the electrodes, especially the one of WE is of paramount importance, in order to achieve the best performances during electrochemical analysis. Traditionally Mercury electrodes were applied, but the latest findings on its toxicity, volatility and its tricky disposal^[21] push forward the need to identify mercury-free devices^[19]. The most attractive candidates to replace mercury based electrodes appear to be noble metals - particularly platinum (*Pt*) and gold (*Au*) - and carbon based materials^[23]. They offer simple fabrication through photolithographic processes with performances in terms of limits of detection and repeatability perfectly suitable for trace element detection, in the order of few $\mu\text{g}/\text{L}$ (or *ppb*).

2.4. Classification

A classification of electrochemical techniques applied for heavy metal detection can be made on the basis of the nature of the excitation signal and the corresponding response provided by the analyte in aqueous solution. They are defined as amperometric, potentiometric, voltammetric, impedance measurements, coulometric and electrochemiluminescent techniques as the target ion produces a change in voltage, current, electrical impedance, charge or electrochemiluminescence respectively.

In the majority of the actual applications the relevant parameters are the current or the potential of the system; either one of them is controlled while the changes in the other one are monitored^[16].

Figure 4 provides an overview on the classification of electrochemical techniques applied in the field of heavy metal detection.

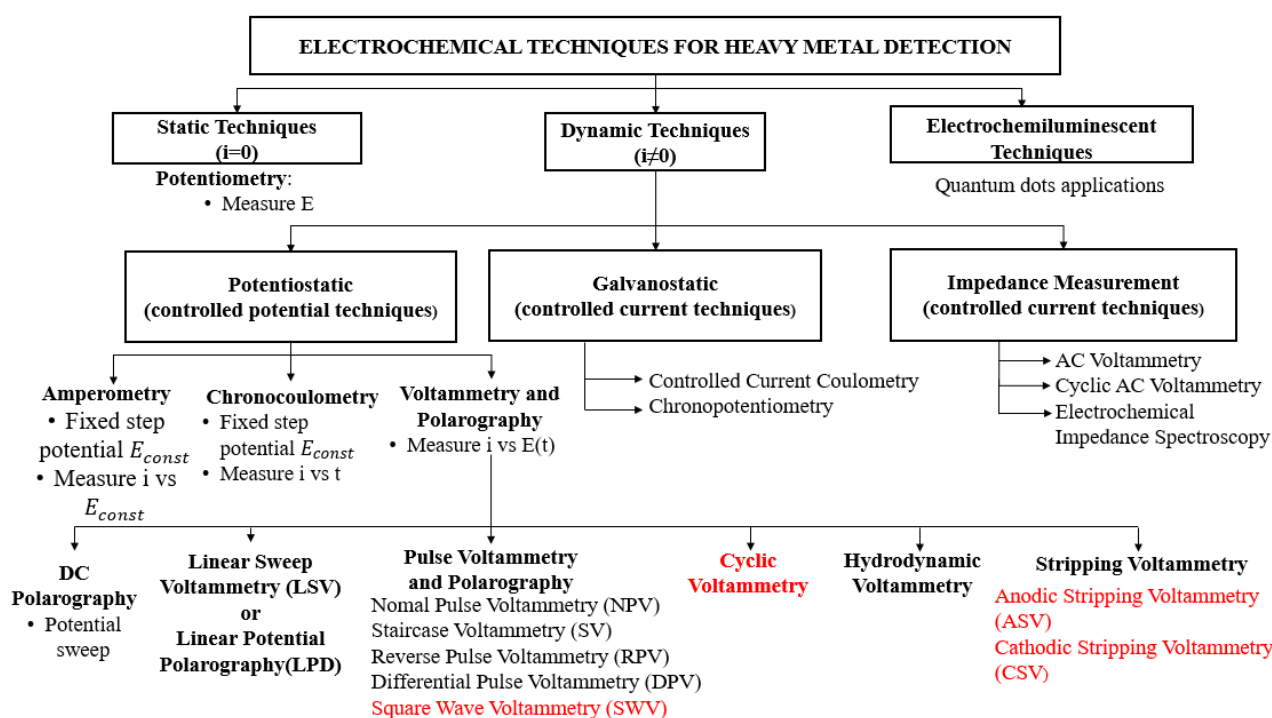


Figure 4-Classification of the electrochemical techniques applied for the detection of metal ions, with the ones considered in this study highlighted in red; adapted with permission from reference^[23].

As will be discussed in the following paragraphs, a serial combination of different techniques, namely stripping voltammetry followed by a square wave scanning, leads to the best analytical performances for trace metal detection.

2.5. Potentiostatic techniques for trace element detection

Potentiostatic techniques implicate the control of the potential at the electrode-electrolyte interface. Ideally this would coincide with the potential gap between RE and WE, but the presence of the unavoidable ohmic drop due to the solution resistance interposed causes it to be slightly different. The instrument involved in this kind of technique is the potentiostat; to achieve the purpose of keeping a defined potential difference between RE and WE, the potentiostat drives the proper current at CE. An example of a basic potentiostatic circuitry is shown in *Figure 5*.

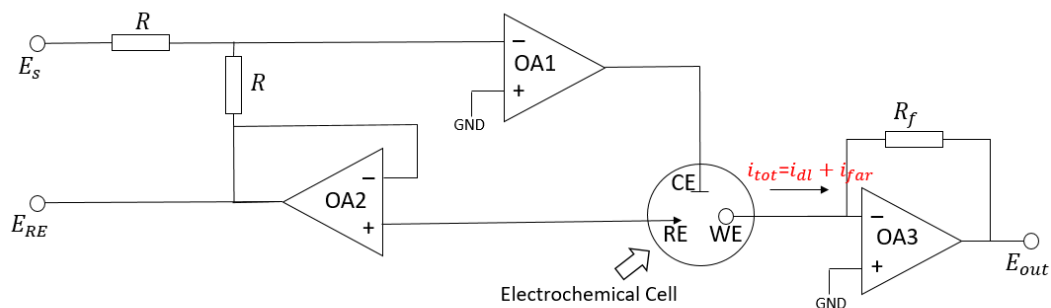


Figure 5-Basic schematic of a potentiostat showing the electrochemical cell with the three electrode setup. The relevant phenomena occur at the electrode-electrolyte interface, on top of the working electrode (WE).

Some important characteristics should be pointed out:

- 1) The Working Electrode (**WE**) is effectively held at virtual ground by the operational amplifier OA3
- 2) The job of the Counter Electrode (**CE**) is to supply the current and therefore the proper voltage needed to sustain the reaction of the target analyte at the Working Electrode (**WE**).
- 3) The Reference Electrode (**RE**) has a bivalent purpose of measuring the potential of the solution near the Working Electrode (**WE**) and supply a potential reference point.
- 4) The operational amplifier OA2 is in the voltage-follower configuration therefore acting as a buffer for the reference electrode (it reports at the output the potential of the reference electrode with a low output impedance)

- 5) The feedback loop of the operational amplifier OA1 includes the solution with the target analyte.
- 6) The voltage at the output of OA1 will make the current flowing through the counter electrode equal to the one that passes through the working electrode (WE) and will maintain the potential vs the reference electrode at the proper point.

Among potentiostatic methods the ones that provide the best accuracy and sensitivity for heavy metal ions detection are the voltammetric ones. They are based on time varying voltage excitation waveforms $E(t)$ and track the corresponding current. The relevant function will be the resulting voltammogram, a current-voltage (i vs $E(t)$) curve. These methods are adapted in order to maximize the rejection of the background current not related to the concentration of the target analyte and to lower the limits of detection (LOD)^[24]. The next sections will clarify how these methods can be coupled for the speciation of complex samples.

2.6. Stripping voltammetry: the importance of preconcentration

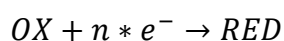
The quantitative analysis of trace elements in diluted samples with complex matrices from various settings (environmental, clinical or industrial) demands a preconcentration step prior to the effective quantification. A simple and reagent-effective way to achieve this task is the electrolytic deposition of the analyte^[17].

During the preconcentration step the target element is deposited onto the working electrode; in the stripping phase it is afterwards oxidized or reduced back into the solution and the corresponding response is recorded. These process provides a double advantage: on one side it separates the analyte from the complex matrix and allow for the detection of target elements near the LOD of the analytical method applied.

2.7. Square wave voltammetry: rejection of the background current

As stated in the previous paragraphs, voltammetric techniques are related to the current-time signal that is generated at an electrode in a controlled potential experiment, provided that faradaic processes involving the target analyte occur. The current is the derivative of the charge over time and theoretically it represents the rate at which the charge-transfer happens at the electrode-sample interface.

As pointed out in the introductory chapter, the key word in electrochemical techniques is REDOX reaction :



The manifestation of the sharp concentration profiles that vary with time at the electrode-solution interface under potential control, is the measured current itself.

Square Wave Voltammetry is the evolution of pulse voltammetric techniques based on a potential excitation waveform represented by the superimposition of a small amplitude square wave over an ideal staircase. The typical potential control exerted during this method is depicted in *Figure 6*.

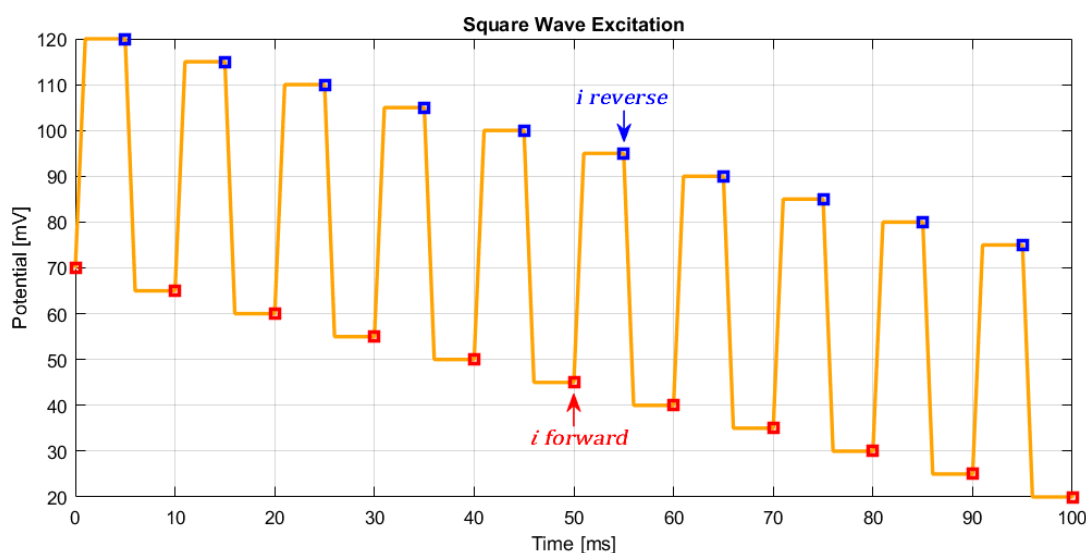


*Figure 6 - Example of Square Wave Excitation Waveform for Cathodic Voltammetry, where the staircase potential is scanned from a positive to a negative value. *i forward* (red dot) represents the forward current sampled after the pulse in the direction of a negative potential, as the underlying staircase, whereas *i reverse* (blue dot) is the current sampled at the end of the pulse in the opposite potential direction with respect to the underlying staircase.*

The corresponding current is sampled twice, after each half wave of the square wave modulation and the resulting net current is a real differential signal between the forward current i_f (red dot in *Figure 6*) and the reverse current i_r (blue dot in *Figure 6*), as shown in *Eq.2.4* :

$$\Delta i = i_f - i_r \quad (2.4)$$

As the definition of these two quantities might be misleading, it is important to clarify that the forward current i_f is the one assessed at the end of the half pulse in direction of the staircase potential, whereas the reverse current i_r is the one sampled after the half pulse in the potential direction opposite to the variation of the underlying staircase.

The voltammogram generated by applying this analytical technique provides the best rejection of the background currents. These unwanted signals arise from various components including:

- 1) Charging current derived from the double layer capacitance C_{dl} , that might be caused either by a changing in the double layer capacitance or by a changing in the potential, as shown by *Eq.2.5*

$$i_{dl} = \partial Q_c / \partial t = \partial (C_{dl} V) / \partial t = \partial C_{dl} / \partial t + \partial V / \partial t \quad (2.5)$$

where i_{dl} is the capacitive current due to the presence of the double layer, Q_c is the charge accumulated on the plates of the capacitance, C_{dl} is the double layer capacitance itself, that builds up as a consequence of charge separation and V is the voltage drop across the double layer capacitance

Considering the electrical equivalent depicted in *Figure 3*, the capacitive current i_{dl} sums to the faradaic component i_{far} but thanks to the velocity of the square wave application it rapidly decays to zero during both the forward and the reverse scanning and its effect on the measured current i_{tot} is minimized

- 2) Current arising from convective mass transport. The rejection of this part is achieved by short square wave periods τ , compared to the time required for convective transport to take place.

Moreover, the differential nature of square wave voltammetry allows to get rid of all of the possible background components that turn out to be equal during the forward and reverse sampling and therefore easily depleted.

These considerations point out how a proper tuning of the square wave parameters improves the capabilities of this technique. As presented in *Figure 7* they include:

- Square Wave Amplitude E_{sw}
- Amplitude of the step potential ΔE_s
- Square Wave Period $\tau = 2t_p$, where t_p =period of the traditional pulse wave

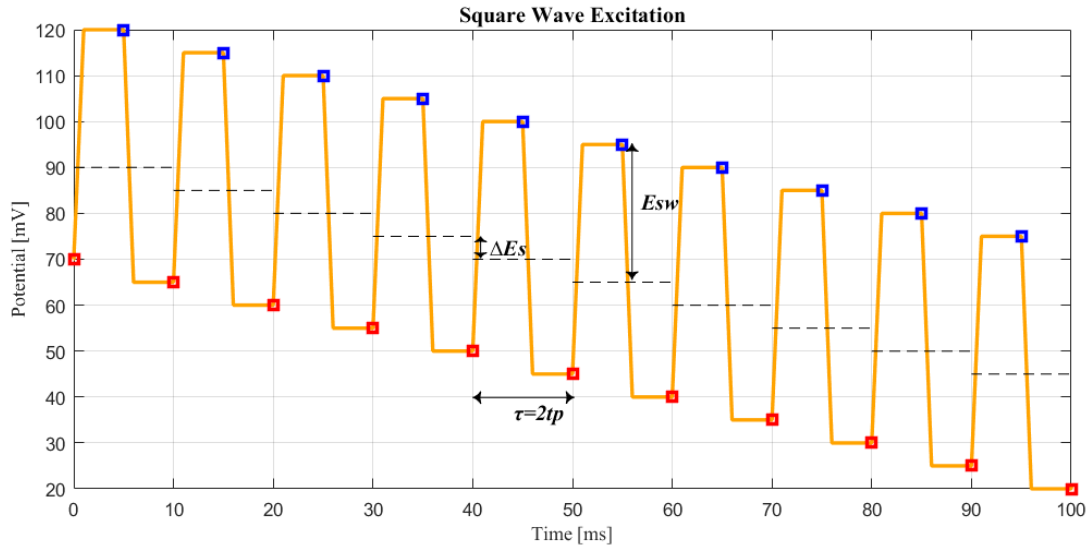


Figure 7-Example of Square wave Excitation Waveform for Cathodic Voltammetry with highlights of the square wave parameters E_{sw} = square wave amplitude, $\tau = 2t_p$ = square wave period, ΔE_s = step potential

It has been established^[19] that, for a redox reaction in the form exemplified by Eq.2.6, to maximize the sensitivity of the method, the relevant parameters should be selected according to the principles summarized in TABLE I.



TABLE I-SQUARE WAVE PARAMETERS

SQUARE WAVE PARAMETER	VALUE
SQUARE WAVE AMPLITUDE E_{sw}	$10mV/n \leq E_{sw} \leq n * 50mV$
STEP POTENTIAL AMPLITUDE ΔE_s	$8mV/n \leq \Delta E_s \leq 12mV/n$
SQUARE WAVE PERIOD $\tau = 2t_p =$ $1/frequency$	$10ms \leq \tau \leq 100ms$

Some important remarks on each of the above-mentioned parameters are worth to be underlined.

First of all, the amplitude of the square wave E_{sw} should be large enough that each half wave is able to produce the oxidation or the reduction of the target analyte at the electrode-solution surface, thus ensuring that the net current is larger than the single reverse or forward current because it is the difference of the two^[15,22]. A decrease in the square wave amplitude reduces the net peak current without improving the resolution; on the other side an excessive increase in the square wave amplitude may broaden the net current peak.

Moreover, the amplitude of the step potential ΔE_s must be confined into a precise interval in order for the small amplitude approximation of the staircase as a combination of infinitesimal potential steps to be valid.

With regard to the last parameter, τ , it is mandatory to consider that the current i measured at each pulse is given by the Equation (2.7)^[25]

$$i \propto \frac{1}{\sqrt{t_p}} = \frac{1}{\sqrt{\tau/2}} \quad (2.7)$$

Decreasing the period τ of the square wave (and consequently increasing its frequency) increases each single current peak; in addition some frequencies must be avoided in order to minimize the effect of the 50Hz (in Europe) or 60Hz (in US) electric noise of the supply AC current.

It is clear that the association of preconcentration strategies (deposition phase) followed by square wave excitation (stripping phase) allows for the rapid, sensitive and selective measurement of several analytes; moreover, the progresses of microelectronics and data processing techniques enabled the integration of the simple potentiostat into disposable devices as opposed to the gold standard techniques presented at the beginning of this chapter.

2.8. SWASV vs SWCSV

Two basic square wave approaches are available for the described purposes:

- 1) SquareWave-Cathodic Stripping Voltammetry
- 2) SquareWave-Anodic Stripping Voltammetry

Their application depends upon the properties of the target analyte and is related to the interferences with the hydrolysis of water molecules. Their major characteristics are reviewed in TABLE II.

TABLE III- CHARACTERISTICS OF SWASV VS SWCSV.

SWASV	SWCSV
<p>ANALYTE: Standard Potential of the redox reaction involving analytes more positive than the standard potential for hydrolysis of water ($\sim -1.2V$)</p>	<p>ANALYTE: Standard Potential of the redox reaction involving analytes near the standard potential for the hydrolysis of water ($\sim -1.2V$)</p>
<p>STRIPPING PHASE: net oxidation of the analyte back into the solution Forward Potential: favors oxidation Reverse Potential: favors reduction</p>	<p>STRIPPING PHASE: net reduction of the deposited analyte back into the solution Forward Potential: favors reduction Reverse Potential: favors oxidation</p>
<p>STRIPPING CURRENT: Forward Current: Anodic Current Reverse Current: Cathodic Current Net Differential Current: Anodic Current</p>	<p>STRIPPING CURRENT: Forward Current: Cathodic Current Reverse Current: Anodic Current Net Differential Current: Cathodic Current</p>

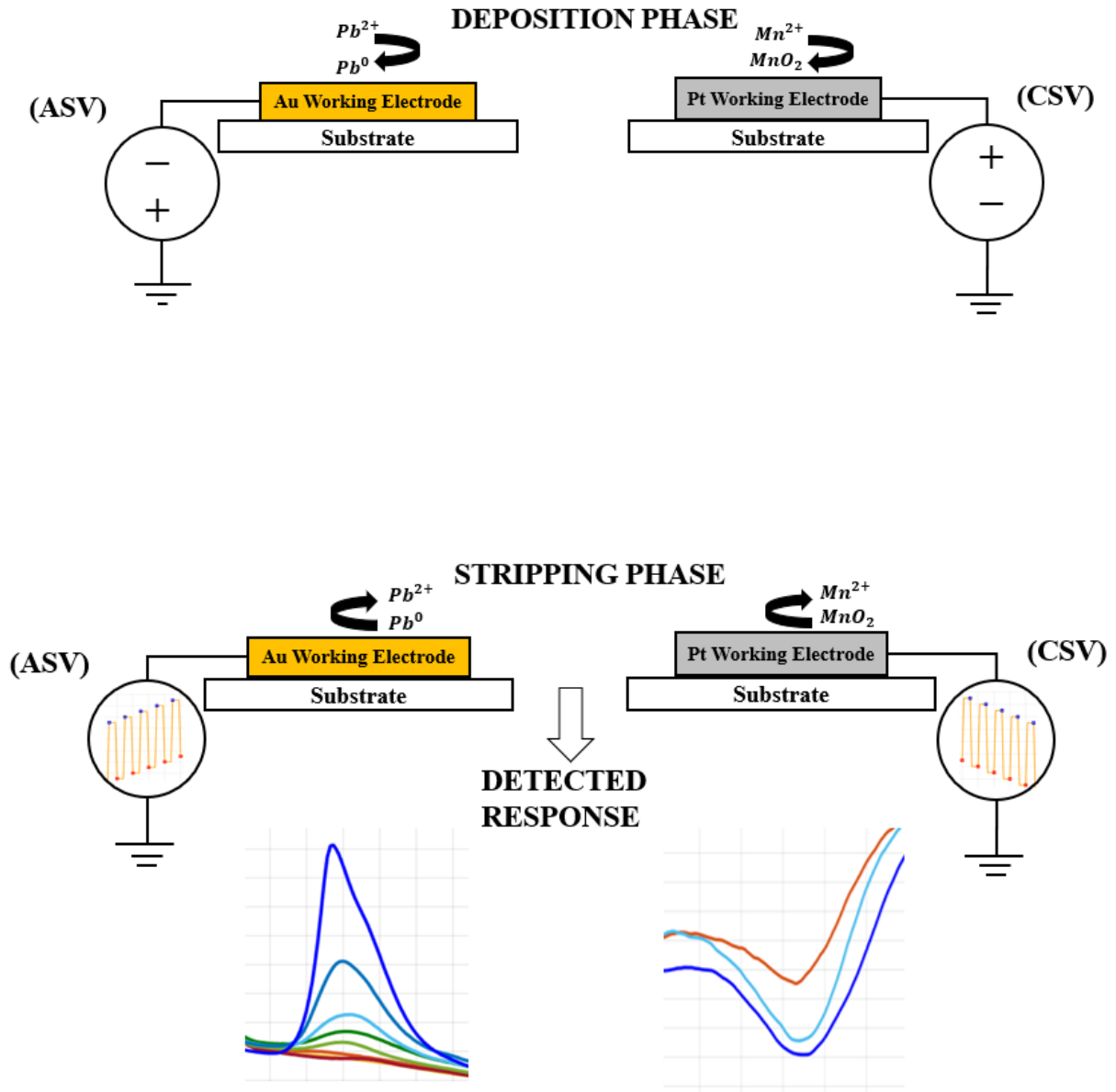


Figure 8-Comparison between Anodic (left) and Cathodic (right) stripping voltammetry during the two phases of the analysis. Top panel shows the deposition phase when the target is concentrated onto the working electrode – Bottom panel pictures the stripping phase during which the effective signal is acquired

CHAPTER 3

MATERIALS AND METHODS

3.1. Reagents

Manganese (Mn) and Lead (Pb) solutions at tested concentrations are made from standard solutions for Atomic Absorption Spectrometry (AAS) at initial concentrations of 1000mg/L (10^6 ppb, parts per billion) in 2-5% Nitric Acid (HNO_3) purchased from Acros Organics (part of ThermoFisherScientific, Waltham, MA USA 02451). For dilution of Pb solutions and initial testing on Mn solution of Sodium Acetate Buffer (AB) at pH 5.2 ± 0.1 ($25^\circ C$), 3M are bought from Sigma Aldrich, St. Louis, MO USA 63103. Solution of Borate Buffer 20X concentrate for initial testing on Mn is purchased from ThermoFisher Scientific, Waltham, MA USA 02451, and diluted 20 times with deionized water ($DI H_2O$) in order to obtain 50mM Borate Buffer pH8.5.

For electroplating the Ag/AgCl reference electrode and treatment (cleaning) of the sensors the following reagents are employed:

- Sulfuric acid (H_2SO_4) solution at 0.05M, made by diluting in $DI H_2O$ pure H_2SO_4 , ACS grade.
- Silver (Ag) solution plating, Silver Cylless II RTU purchased from Technic Inc, Cranston, RI USA 02910
- Potassium Chloride (KCl) solution at 0.1M, made by dissolving $KCl_{(s)}$ in $DI H_2O$

For sample preparation the listed chemicals are required:

- Nitric acid (HNO_3) trace metal grade
- Hydrogen Peroxide (H_2O_2) solution at 30% in H_2O
- Sodium Hydroxide ($NaOH$) solution at 5M or 12M, made from $NaOH_{(s)}$ diluted in $DI H_2O$

Unless otherwise specified, all of the above mentioned chemical species are purchased from FisherScientific (part of ThermoFisherScientific, Waltham, MA USA 02451).

Human whole blood samples are purchased in 10mL tube from ZenBio Inc, Research Triangle Park, NC 27709. All of them are treated with dipotassium ethylenediaminetetracetic acid (K_2 – *EDTA*) as anticoagulant.

3.2. Sensors

The sensors employed in this work are purchased from Micrux Technologies, Oviedo, Asturias Spain 33006.

Figure 9 shows an inset of the Platinum sensor with the three electrodes in evidence.

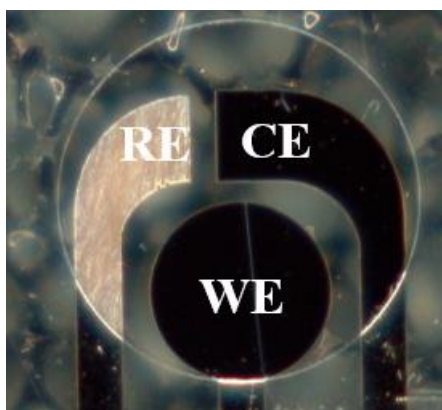


Figure 9-Inset on the active surface of the Platinum sensor - WE=WorkingElectrode, CE=CounterElectrode, RE=ReferenceElectrode

Both for Mn and Pb detection the same model of sensors ED-SE1 is used. The only difference between the sensors applied for the detection of the analytes lies in the material of the top layer: Gold (*Au*) for Pb detection and Platinum (*Pt*) for Mn detection. Their relevant features are listed in TABLEIII.

TABLE III- SPECIFICATIONS OF THE APPLIED SENSORS ED-SE1.

FEATURE	DESCRIPTION
ELECTRODE SETUP	3 electrode architecture: <ul style="list-style-type: none"> • WE • RE • CE
SENSOR DIMENSIONS	10x6x0.75 mm
AREA WORKING ELECTRODE	$\pi(0.5\text{mm})^2 \cong 7.85 * 10^{-7}\text{mm}^2$
PROTECTIVE LAYER	SU-8 layer with a 2mm circular opening
SUBSTRATE MATERIAL	Glass
SEED LAYER MATERIAL	50nm Ti
TOP THIN FILM MATERIAL	<ul style="list-style-type: none"> • 150nm Au for Pb detection • 150nm Pt for Mn detection

Figure 10 shows an overview of the setup used during all of the experiments, with the electrodes positioned inside the interface provided by the Micrux for the connection with the potentiostat.

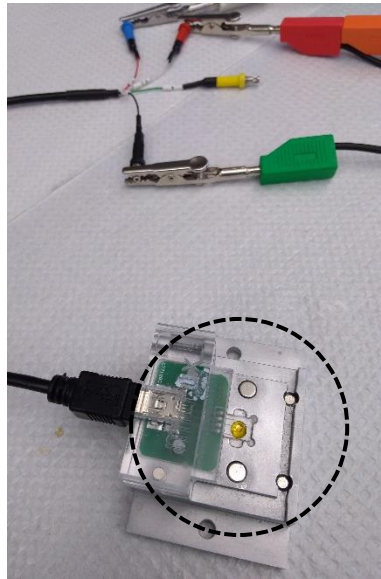


Figure 10-Overview of the setup during an experiment with a 10 μ L droplet of treated human blood , on the background are depicted the connections of the three electrode system to the potentiostat

Prior to any treatment or analysis all of the sensors are electrochemically cleaned with at least 12 cycles of cyclic voltammetry in the potential range -1.3V to +1.3V with 0.05M sulfuric acid (H_2SO_4). The same procedure is applied also after each usage.

For the creation of the *Ag/AgCl* Reference Electrode (RE) on both the Au and the Pt sensors the electroplating technique is applied, following the protocol optimized in a previous work done by collaborators^[16]. Nevertheless it is important to briefly describe the overall procedure.

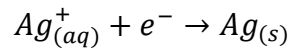
Electroplating can be defined as the application of a metal coating to a metallic or other conductive surface by an electrochemical procedure.

In this study a two-step process is performed:

1. Electrodeposition of silver (Ag) on the reference electrode

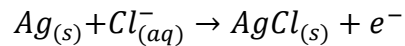
During this step the reference electrode is made the cathode of the electrolytic cell (i.e. the terminal at which reduction occurs) and deposition of silver from the silver based solution is achieved; a

cathodic current $i_c = 12.55\mu A$ is provided by the potentiostat through a chronoamperometric experiment for $t_c = 240s$.



2. Electrodeposition of chloride (Cl) on the reference electrode

The reference electrode coated with electrodeposited Ag is then chloridized in 1M KCl by reversing the electrolytic cell (i.e. the reference electrode RE coated with $Ag_{(s)}$ is made the anode of the cell, where the oxidation occurs). An anodic current $i_a = 12.55\mu A$ is provided by the potentiostat through a chronoamperometric experiment for $t_a = 120s$.



It is important to point out that the time for the chloridization (120s) is half of the one applied for the deposition of Ag (240s) in order to have a final molar ratio Ag:AgCl of 1:1.

Figure 11 plots the chronopotentiogram (or the voltage-time curve) provided by the reference electrode with respect to ground during the chloridization phase; from that it is possible to infer that the potential given by the plated electrode is stable after the final steps of electroplating.

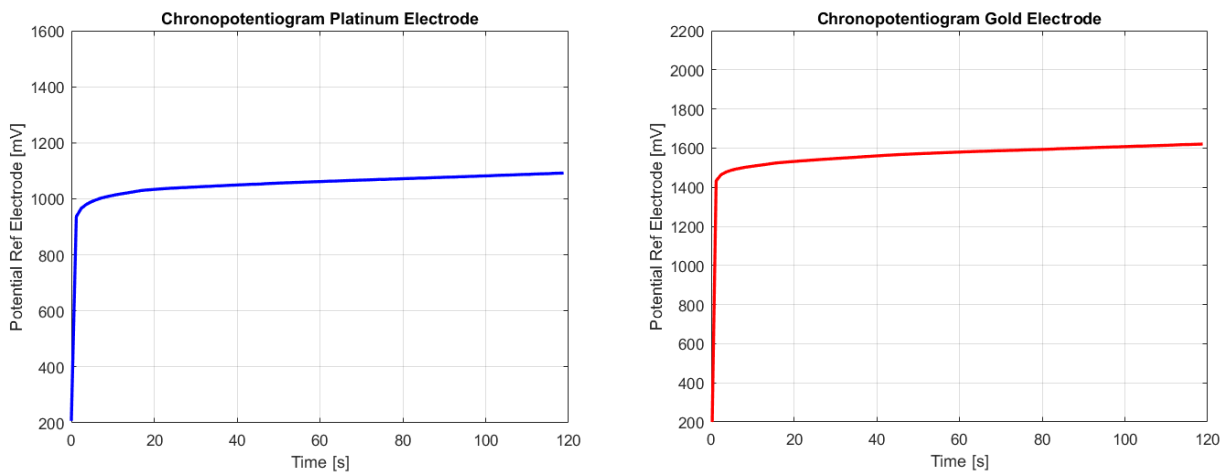


Figure 11- Chronopotentiogram (Voltage-Time curve) of the Platinum (left) and Gold (right) electrodes during the chloridization step of electroplating.

It is also interesting to visualize the color changes that occur on the reference electrode surfaces after each stage, as depicted in *Figure 12*

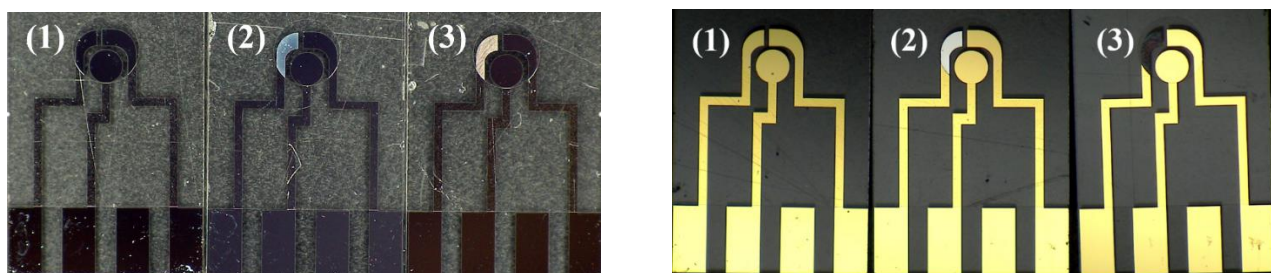


Figure 12- Platinum (left) and Gold (right) electrodes after each phase of electroplating- (1) Bare Electrode before any treatment, (2) Electrode after Ag deposition, (3) Electrode after Cl deposition.

3.3. Whole blood digestion

One of the most important and most critical passages of the detection of trace metal elements in biological samples is the preparation of the sample itself. Acid digestion technique, derived from sample pre-treatment required for ICP-MS, is applied with some important variations that make it more feasible in an unspecialised laboratory and in the next future might allow its integration into a microfluidic device.

The basic purpose of acid digestion is the decomposition of any organic matter^[18], in order for the trace elements to be detected to recover their ionic form. For whole human blood this includes the breakdown of all the cells and proteins which the analytes are bound to. The protocol developed originates from a previous work done by C.Rusinek et al.^[19,36]. In order to reduce the dilution of the sample, that is found to be a determining factor in trace metal detection, a first revised procedure has been realised by Dr.Thushani Siriwardhane (named **PROTOCOL A**). This approach works very well with bovine blood, but when performed on human blood several issues come out and just from the first step with the addition of HNO_3 is noticed the presence of a large amount of white residuals, attributed to formation of protein aggregates that are not destroyed by nitric acid. A revised protocol

(named **PROTOCOL B**), that takes into account a slight increase in the volume of nitric acid is developed. TABLE IV provides an insight on the two different schemes with highlights of the major differences.

TABLE IIV-DIGESTION PROCESS: PROTOCOL COMPARISON

PROTOCOL A	PROTOCOL B
1) SAMPLE: 250 μ L Human Blood	1) SAMPLE: 250 μ L Human Blood
2) Addition of 175 μ L of trace metal grade Nitric Acid (HNO_3) to each digestion vial	2) Addition of 250 μ L of trace metal grade Nitric Acid (HNO_3) to each digestion vial
3) Vials in the Hotblock at 90°C for 30 minutes to perform pre-digestion	3) Vials in the hotblock at 90°C for 30 minutes to perform pre-digestion
4) Increase temperature up to 120°C for 90 minutes to perform acid digestion	4) Increase temperature up to 120°C for 90 minutes to perform acid digestion
5) Let the sample cool down at room temperature	5) Let the sample cool down at room temperature
6) Additon of 87.5 μ L of 30% H_2O_2	6) Additon of 110 μ L of 30% H_2O_2
7) Temperature of the hotblock at 120°C for 90 minutes	7) Temperature of the hotblock at 120°C for 90 minutes
8) Let the sample cool down at room temperature before pH adjusting	8) Let the sample cool down at room temperature before pH adjusting

It should be highlighted that the first 30 minutes in the hotblock, after the addition of HNO_3 are required for the pre-digestion of the heavy organic matrix and the subsequent combination with H_2O_2 allows to regenerate HNO_3 and therefore maximize the capabilities of the method performed without highly specialized equipments such as digestion microwaves traditionally applied before ICP-MS testing. Markers of a proper digestion can be considered a yellowish and transparent color of the treated sample, without any particulate matter.

After acid digestion the samples present a strong acidic pH that needs to be adjusted in order not to damage the sensors and affect the success of the detection. This stage is carried out with the dropwise addition of a strong base (typically $NaOH$ solution at 5M or 12M). At the end of this step the sample is ready for the measurement. *Figure 13* shows two examples of treated blood samples before (right vial) and after pH adjusting (left vial). It is interesting to notice the change in color

between the two, remark that might make feasible to the colorimetric check of pH for future automatization of the overall procedure.

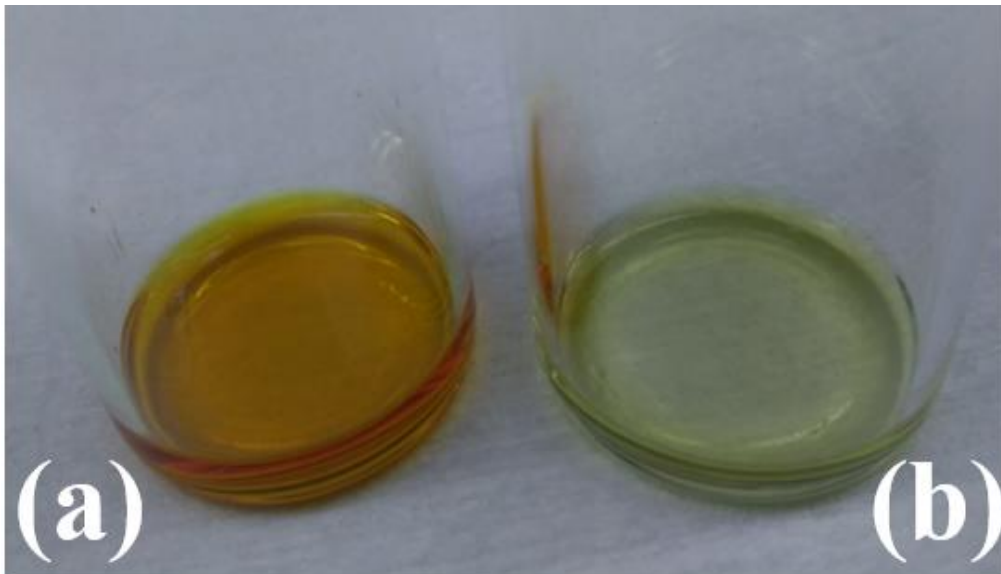


*Figure 13-Blood samples after acid digestion following **PROTOCOL B**- (a) Blood sample after pH adjusting with 12M NaOH ,pH of the final solution around 5- (b)Blood sample before pH adjusting, highly acidic. Despite the difference in color both of the two samples look transparent and without particulate residuals, indexes of a proper digestion.*

3.4. Standard addition

Standard addition is defined as a calibration method designed in order to overcome the effects of a complex matrix when dealing with analytical samples^[20]. It can be considered as an internal standardization and it is particularly useful for the analysis of biological samples, such as blood, urine or saliva when the sensitivity of a test varies from sample to sample and an external calibration turns out to be unfeasible. When the matrix of the sample can affect the sensitivity of analytical measurements two different effects can occur, namely a ‘rotational or proportional effect’ highly dependent upon the signal (in this case the concentration of the target element) and a ‘translational effect’, independent from the signal and affecting the intercept but not the slope of the calibration curve^[29].

Standard addition allows to overcome the rotational effect and its key steps are:

- 1) measurement of the signal from the unknown sample
- 2) addition of known concentrations of the target analyte to the unknown sample
- 3) measurement of the given signal after each addition
- 4) estimation of the calibration curve through linear regression at least squares
- 5) extrapolation of the unknown concentration in the sample as the absolute value of the x-axis intercept of the estimated calibration curve.

3.5. Software

For data acquisition from the potentiostat the software Aftermath, Pine Research Instrumentation, Durham, NC 27705 USA is used. It provides automatic tools to compute the peak current value and identify the peak position and full width at half maximum (*FWHM*).

For data analysis and generation of the graphs the software Matlab[®], The MathWorks Inc., Santa Clara, CA 95054 USA is employed.

CHAPTER 4

RESULTS AND DISCUSSION

4.1. Lead detection on Au electrodes

As highlighted in *Figure 8* the main actor in Pb detection during SWASV is represented by the following redox reaction that occurs at the electrode-sample solution interface:



with $n = 2$ electrons exchanged

In order to assess the capabilities of gold-based electrodes for Pb determination through Square Wave Anodic Stripping Voltammetry and identify the proper supporting electrolyte, a prior Cyclic Voltammetry analysis is conducted.

Two different supporting electrolyte are tested: Acetate Buffer (*AB*) at pH 5.2, Borate Buffer (*BB*) at pH 8.9. As depicted in *Figure 14 (a)*, Acetate Buffer pH 5.2 turns out to be more stable at negative potentials required for Anodic Stripping of the target analyte and it is therefore chosen as the supporting electrolyte to carry out the study of the performances of the gold sensors. The dashed oval highlights the region where the lead (*Pb*) reduction peak is expected^[21]. It is clear that for anodic methods, where the potential is typically in the negative side ($E(t) < 0V$), the reduction and oxidation of the Au electrode does not impact, since they occur at more positive potentials as represented by the sharp peaks at around +0.4V and +0.8V.

To confirm the capabilities of the applied sensors and locate the lead (*Pb*) reduction peak, cyclic voltammetry in AB pH5.2 is repeated with the addition of 10ppm *Pb* (48.2 μM). As shown in *Figure 14(b)* a well resolved reduction peak is detected at a potential $E_{red} \approx (-0.31 \pm 0.07)V$, mean on $n = 3$ electrodes.

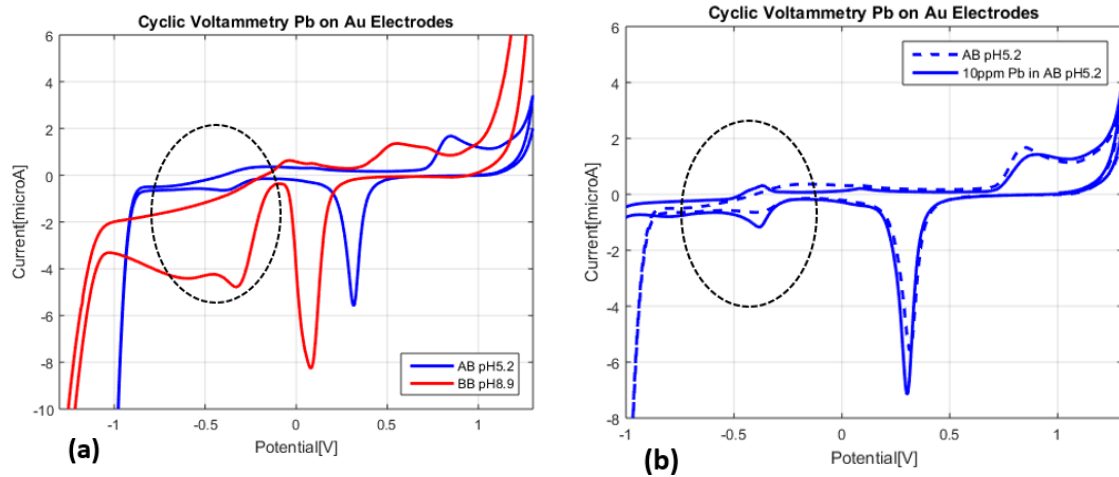


Figure 14-(a) Cyclic voltammetry on Au Electrodes, comparison between Acetate Buffer (AB pH 5.2) and Borate buffer (BB pH 8.9) and (b) Cyclic Voltammetry of Acetate Buffer (AB pH 5.2) alone and with the addition of 10ppm Pb

Provided that the gold-based sensors offer the proper characteristics for lead (*Pb*) detection through SWASV, optimization of the analytical parameters in standard solution is performed.

4.2. Optimization of the SWASV parameters

As highlighted in CHAPTER 2, where a theoretical overview of electrochemical techniques is presented, the most important parameters that affect the measurement in square wave stripping methods (both ASV and CSV) are the following ones:

- DEPOSITION PHASE: deposition potential, deposition time
- SQUARE WAVE STRIPPING: square wave amplitude E_{sw} and square wave period $\tau = 2t_p = 1/\text{frequency}$

Provided that , in order for the small amplitude approximation of the small amplitude signal to hold^[13], the step potential ΔE_s must be confined inside a precise interval , $4mV \leq \Delta E_s \leq 6mV$,it is not taken into account as a relevant parameter to be optimized and an intermediate value of $\Delta E_s = 5mV$ is chosen.

Moreover, in practical experiments also the pH of the supporting buffer electrolyte is thought to be a determining factor in the performances of the measurement and a remark on that should be made.

Its importance is more related to the nature of target element itself, in this case lead (*Pb*) rather than to the material of the electrode. Previous works by C.Rusinek et al.^[21] have demonstrated that the value that ensures lower signal variability, best peak sharpness and stable response lies in between pH 5 and pH 5.5, therefore Acetate Buffer at pH 5.2 is selected for the analysis.

To provide consistency with the current threshold for elevated *Pb* levels in human blood, fixed at $\leq 180\text{ppb}$,^[34] all the experiments are carried out with a sample of $10\mu\text{L}$ of 100ppb ($0.48\mu\text{M}$) *Pb* in Acetate buffer pH5.2. Triplicate experiments are performed for each parameter to define the mean value μ , the standard deviation σ and the coefficient of variation $CV\% = (\sigma/\mu)*100$.

Each parameter is thought to affect the response independently from the others and separate analysis are performed.

- **Deposition phase**

The first fundamental variable considered is the deposition potential, at which WE is held during preconcentration. This parameter is scanned from $E_{dep} = -1200\text{mV}$ up to $E_{dep} = -600\text{mV}$ with deposition a time $t_{dep} = 300\text{s}$. At deposition potentials $E_{dep} \geq -700\text{mV}$ no detectable signal is obtained. As *Figure 15* depicts, at deposition potentials $-1000\text{mV} \leq E_{dep} \leq -700\text{mV}$ double stripping peaks are observed, at $E_{peak1} \sim -420\text{mV}$ and $E_{peak2} \sim -100\text{mV}$. This is in accordance with literature^[26,27], supporting the theory of the underpotential deposition (UPD) of Pb at gold or silver electrodes at relatively short deposition times. This concept can be expressed as the stripping of the target metal into two different steps. Two distinct phases of the deposited metal (*Pb*) can be identified: a metallic monolayer and a superimposed layer due to the deposition of the metal in the bulk solution. After deposition has occurred first the bulk deposit is stripped back into solution (E_{peak1}) and then the underlying monolayer of *Pb* is oxidized back into solution (E_{peak2}). Deposition potentials $E_{dep} \leq -1100\text{mV}$ are not preferable due to their proximity to the redox potential of water molecules and possible degradation of the working electrode surface that impacts on the

reproducibility of the signal in various cases and significantly shifts the stripping peak to more negative values $E_{peak} \sim -650mV$..

For the proposed application on human blood testing, precision is one of the major parameter that must be taken into account and therefore the selected deposition potential is $E_{dep} = -1100mV$ which leads to the minimum coefficient of variation $CV\% = 15\%$. Moreover, at deposition potentials $E_{dep} \leq -1200mV$ oxidation of the gold electrodes occurs randomly, visually verifiable from a change in the color at the surface of the counter electrode.

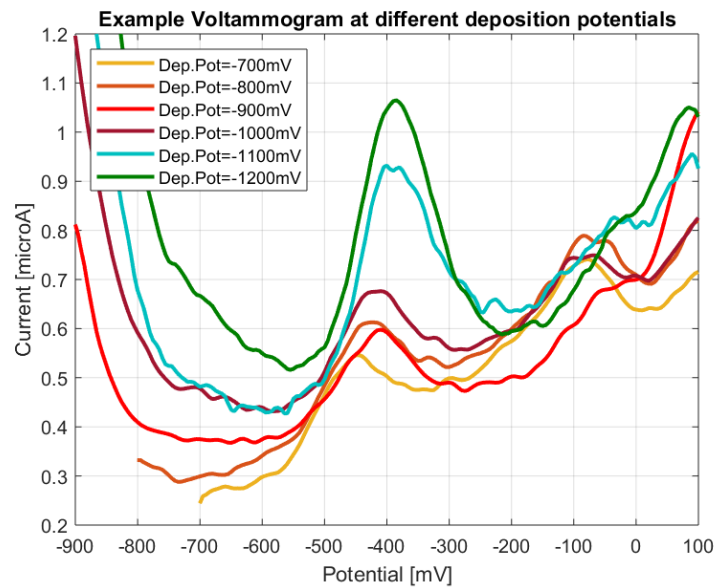


Figure 15-Example of voltammograms obtained at different deposition potentials; for potentials in the range $-1000mV$ - $700mV$ double peaks are observed, leading to a significant decrease in the signal.

The next parameter taken into account for optimization is the deposition time. This variable is scanned at 120s, 180s, 300s, 600s, 900s, 1200s, 1500s.

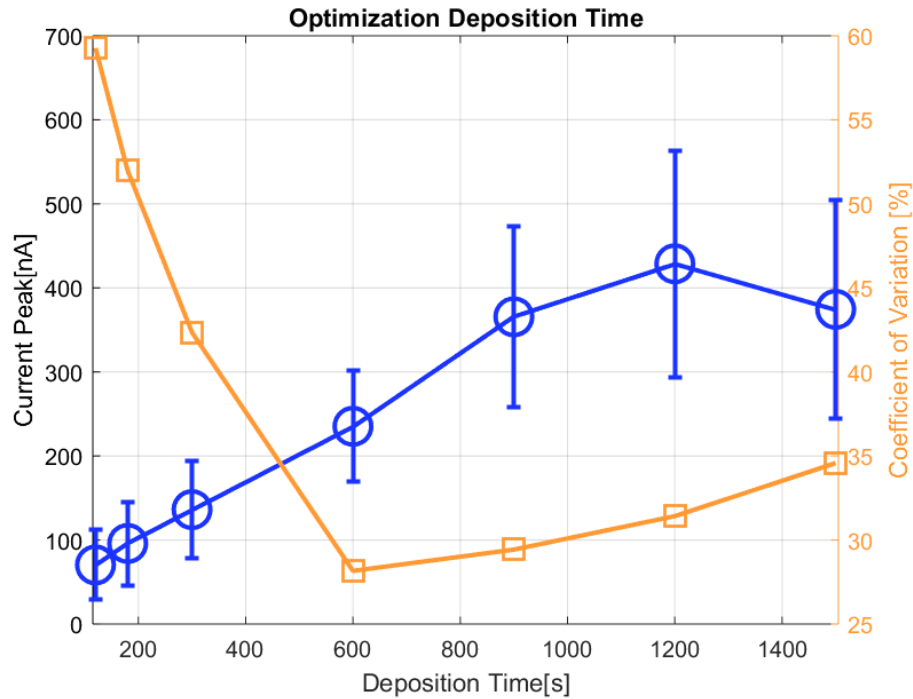


Figure 16-Current peaks and CV% as a function of the deposition time evaluated at 120s,180s,300s,600s,900s,1200s and 1500s

From Figure 16 it seems that the signal continuously increases up to a deposition time $t_{dep} = 1200s$, but so does the standard deviation. In accordance with the need for a rapid on-the-field application, the selected preconcentration time is $t_{dep} = 600s$. For further confirmation of the choice a paired t-test on the equality of means (with the assumption of unequal variances) is conducted by comparing the mean values (computed on three measurements) of the couples 300s-600s ,600s- 900s and 600s-1200s. Actually for none of them it is possible to discard the hypothesis of equal means at the 5% level of significance, with p-values of 0.12, 0.16, 0.11, respectively. Yet, a deposition time of 600s is associated to the minimum coefficient of variation and therefore selected as the optimum one.

- **Square wave**

For optimization of the square wave parameters applied during the stripping phase a deposition potential=-0.9V and a deposition time=300s are selected.

Square Wave Amplitude E_{sw} is scanned from $E_{sw} \text{ min} = 17.5mV (< 50mV/n = 25mV)$ to $E_{sw} \text{ max} = 100mV (n * 50mV)$. Experimental results are partially in accordance with the theory,

since at small values of the square wave amplitude reduced current peaks are found, indicating that the reverse pulses are insufficient to cause the reduction of Pb^{2+} .

Increasing the amplitude of the square wave induces a shift of the potential at which the peak is found from $\approx -380mV$ at $E_{sw\ min} = 17.5mV$ to $\approx -450mV$ at $E_{sw\ max} = 100mV$ and to a broadening of the peak, quantifiable in a maximum mean value of the $FWHM=199.1mV$ for $E_{sw\ max} = 100mV$. From *Figure17* it is possible to extrapolate that the optimum value is $E_{sw} = 50mV$, characterized by the best trade-off between the mean signal $i_{peak}=218.5nA$, the mean $FWHM = 136mV$ and the minimum coefficient of variation $CV\% = 31\%$.

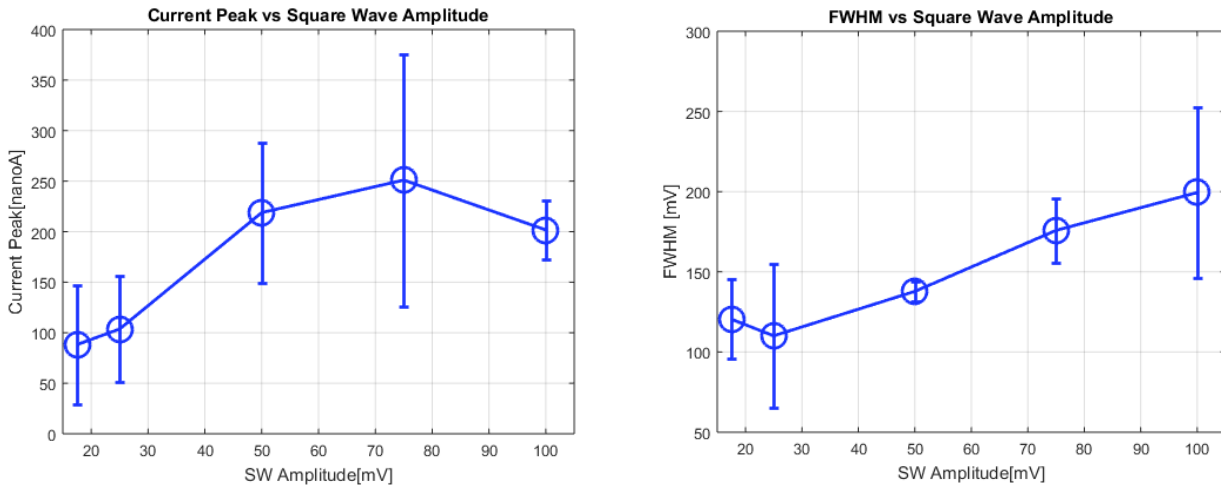


Figure 17-(left) Plot of the Current Peak values vs Amplitude of the applied square wave- (right) Plot of FWHM vs Amplitude of the excitatory square wave. Errorbars represent the standard deviation from the mean value computed over three repetitions.

Square Wave period of the applied excitation waveform is evaluated from 10ms to 100ms.

To identify the ideal value peak current, $FWHM$ (Full Width at Half Maximum, indicative of the sharpness of the peak for a better identification) and $CV\%$ are considered.

Figure17 depicts the obtained results.

It is interesting to underline that, as predicted from Equation (2.7), $i \propto \frac{1}{\sqrt{t_p}} = \frac{1}{\sqrt{\tau/2}}$,

confirming that the value of the current peak decreases with increasing the period of the square

wave and a good linearity ($R^2 = 0.984$) between the peak current and $1/\sqrt{t_p}$ is experimentally found.

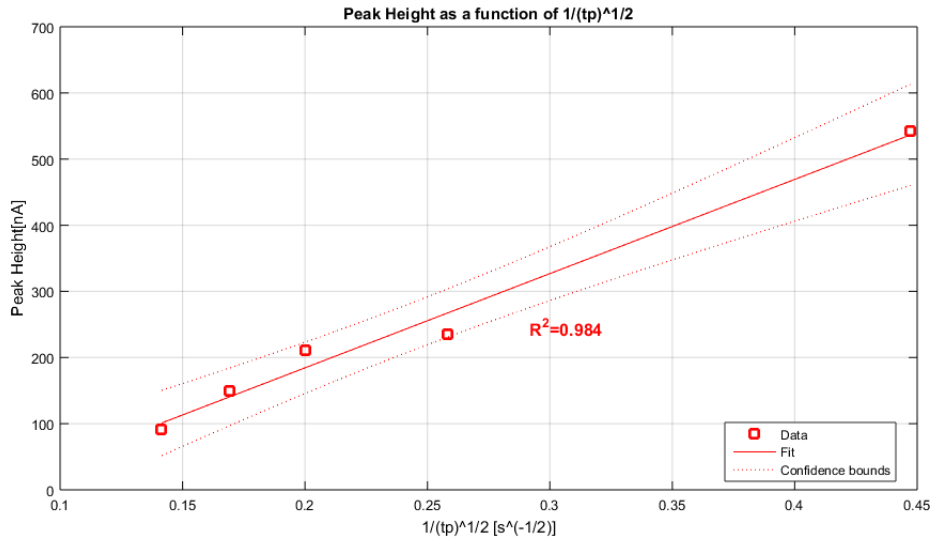


Figure 18-Current Peak [nA] as a function of $1/\sqrt{2\tau}$. Good linearity is in accordance with the theory of square wave voltammetry originally developed by J. G. Osteryoung and R. A. Osteryoung^[19,1]

However, theory and real applications might sometimes be separate and other factors apart from the value of signal must be considered. Although a square wave period $\tau = 10ms$ gives a mean signal $i_{peak} = 542.86nA$, it exhibits a $CV\% = 48.7\%$ and a mean $FWHM = 136.1mV$ and a distortion in the peak signal. The optimal period is therefore selected as $\tau = 30ms$, with a mean peak current $i_{peak} = 235.5nA$, a $CV\% = 22\%$ and a mean $FWHM = 111mV$.

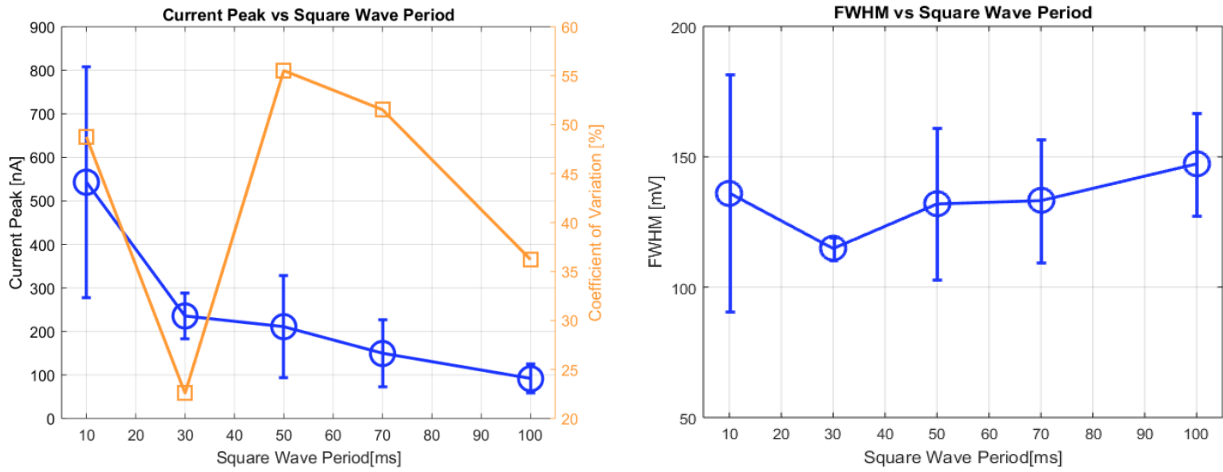


Figure 19-(left) Plot of the current peak values vs Period of the applied square wave- (right) Plot of FWHM vs Period of the square wave. Errorbars represent the standard deviation from the mean value computed over three repetitions.

The overall parameters selected for the following analysis and calibration of Pb on Au electrodes are summarized in TABLE V

TABLE V - OPTIMIZED PARAMETERS FOR SWASV OF PB IN STANDARD SOLUTIONS, ELECTROLYTE: AB PH5.2

PARAMETER	VALUE
DEPOSITION TIME	600s
DEPOSITION POTENTIAL	-1.1V
SQUARE WAVE AMPLITUDE	50mV
SQUARE WAVE PERIOD	30ms
STEP POTENTIAL	5mV

4.3. Calibration

Once the optimum parameters are selected, it is possible to define a calibration curve and assess the limit of detection (LOD) of the method. This last indicator of performances is defined by the following relationship:

$$LOD = 3 * \sigma / slope \quad (4.1)$$

Where σ = standard deviation of the signal at the lowest detectable concentration (5ppb), repeated on 8 measurements and *slope* =slope of the estimated calibration curve, indicative of the sensitivity of the sensor. This parameters identifies the lowest concentration of the measurand that the sensor is able to detect.

Considering the range of Pb levels in human blood ^[34]a range of 5ppb-1000ppb of Pb in standard solutions is selected. *Figure 16* depicts an example of the voltammograms obtained at different Pb concentrations in AB pH 5.2 standard solutions after subtraction of the baseline given by the buffer alone. In order to avoid any possible contamination for each measurement a different electrode is used.

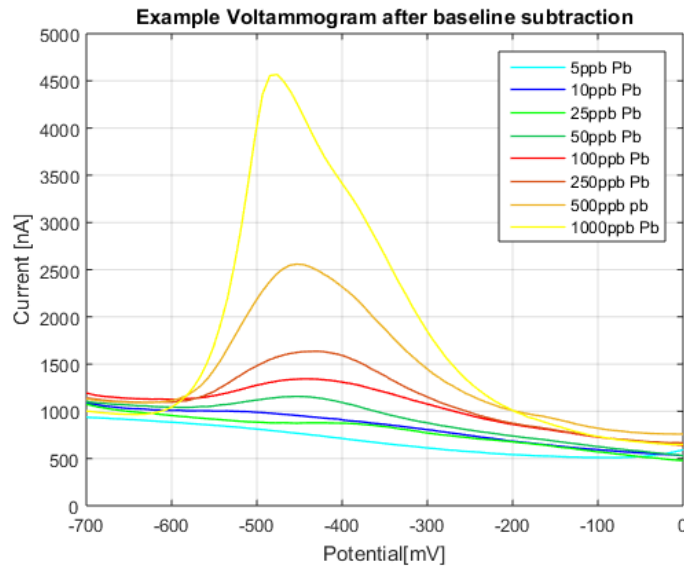


Figure 20-Example of a series of voltammograms obtained in AB pH5.2 at different Pb concentrations, range 5ppb to 1000ppb.

To determine the calibration curve, each experiment is repeated $n=3$ times. Figure 21 shows the obtained calibration curve; it turns out to be $i(nA) = 2.85[Pb(ppb)] + 6.73(nA)$, with a standard deviation for the estimation of the slope, $std_{slope} = \pm 0.098[nA/ppb]$ and a standard deviation for the intercept $std_{intercept} = 36.95[nA]$.

The limit of detection, defined by the Equation (4.1) is $LOD = 7.89ppb$, fully comparable with the performances of carbon or bismuth based electrodes that provide values from 1ppb to 8ppb^[24].

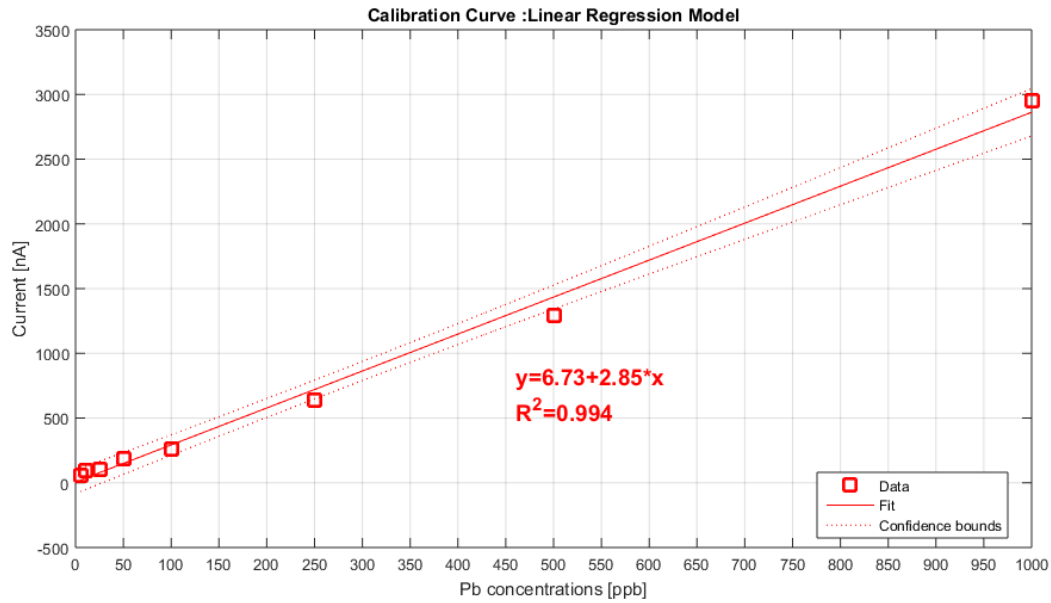


Figure 21-Linear regression model of the calibration curve for the Au sensor for Pb detection in standard solutions. Good linearity is obtained for whole the scanned range, with $R^2=0.994$. Parameters for the SWASV are the optimized ones.

Provided that the LOD is well within the normal range levels of Pb in human blood and particularly is fairly low with respect to the threshold that currently defines Pb levels that require constant monitoring^[33], the gold-based sensors with the chosen parameters are tested on human blood samples.

4.4. Human blood

Blood samples are purchased in 10mL tubes from ZenBio Inc, Research Triangle Park, NC 27709. All of them are treated with dipotassium ethylenediaminetetracetic acid ($K_2 - EDTA$) as anticoagulant. Blood samples tested are collected on 04/11/2018, shipped on 04/12/2018. Digestion, pH adjusting and measurements are performed on 04/17/2018.

Prior to the electrochemical detection the acid digestion treatment described in CHAPTER3 is performed. For all of the samples **PROTOCOL B** is followed.

At the end of the digestion process and pH adjusting the overall dilution factor is $DF_{pt} = 1.3$

For the standard addition two known concentrations are added. The relative amount of volumes and concentrations of Pb are summarised in TABLE VI

TABLE V-STANDARD ADDITION SPECIFICATIONS

VOLUME UNKNOWN SAMPLE	VOLUME OF ADDED STANDARD	CONCENTRATION OF ADDED STANDARD	FINAL VOLUME	DILUTION FACTOR STANDARD ADDITION
100 μ L	10 μ L	- (AB pH5.2)	110 μ L	110 μ L/10 μ L = 1.1
100 μ L	10 μ L	100ppb Pb in AB pH 5.2 (s1)	110 μ L	110 μ L/10 μ L = 1.1
100 μ L	10 μ L	200ppb Pb in AB pH 5.2 (s2)	110 μ L	110 μ L/10 μ L = 1.1
100 μ L	10 μ L	300ppb Pb in AB pH 5.2 (s3)	110 μ L	110 μ L/10 μ L = 1.1

From each sample vial a droplet of $V_{sample} = 10\mu L$ is placed on the sensor for the analysis.

To avoid any contamination from residual material a new sensor is used each time.

The estimated concentration is taken through extrapolation of the intercept with the x-axis and multiplied by dilution factor to recover the original concentration. Two successive repetitions are carried out in order to have a minimum statistical significance of the data.

A first trial quantified the Pb concentration in the blood sample $Unknown_{pb} = 54.73ppb$, a reasonable value compatible with the actual ranges. The estimated regression line, reported in *Figure 22*, turns out to be $i(nA) = 7.76[Pb(ppb)] + 318.97$; this high sensitivity seems promising but care must be taken because a standard deviation of 20.8% is observed.

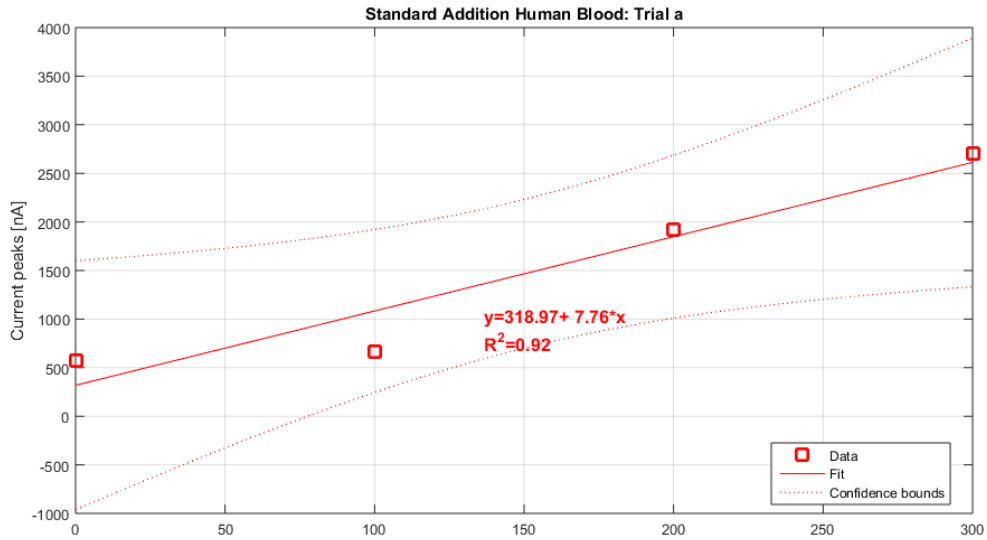


Figure 22-Linear regression model derived from the standard addition on human blood samples. Digestion performed 04/17/2018, first trial

As it is possible to catch from both the panels of Figure 23 in blood samples a peak shift towards more positive values is noticed in each trial from $E_{peak} \sim -390mV$ in standard solutions to $E_{peak} \sim -260mV$ in human blood. This mismatch is attributed to the high concentration of chloride ions present in real samples, which affect the potential of the Ag/AgCl reference electrode. Further testing on standard solutions with added chloride can confirm this hypothesis.

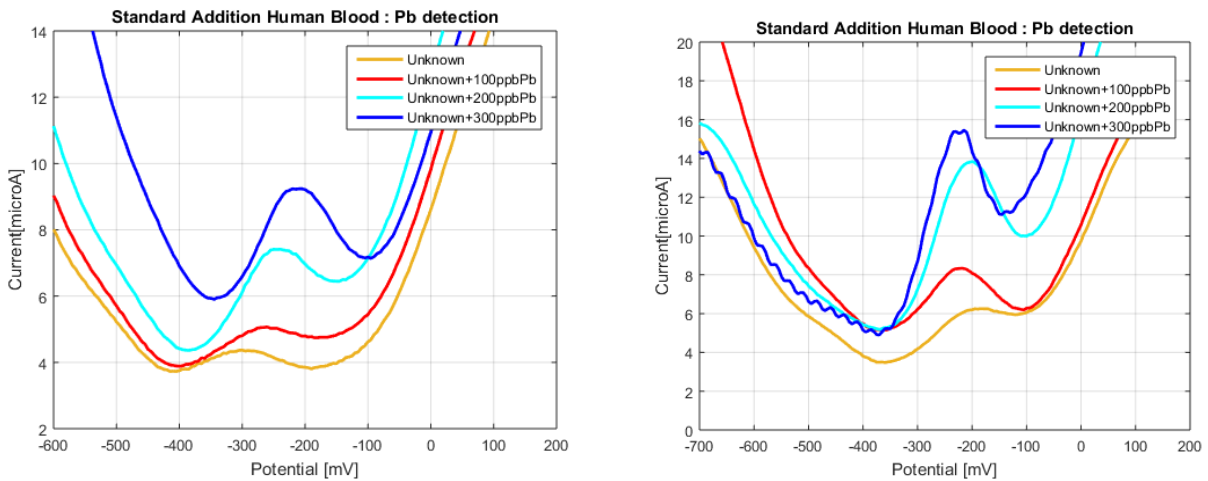


Figure 23-Voltammograms obtained on human blood samples with addition of 3 known concentration of Pb in order to perform the standard addition-Digestion performed 04/17/2018. First trial on the left panel and second trial on the right panel.

The second trial conducted on the same digested blood provided an estimation $Unknown_{Pb} = 72.06 ppb$, with an estimated regression line $i(nA) = 19.63[Pb(ppb)] + 1088.2$ that shows both an increased sensitivity and linearity with respect to the first one, as depicted in *Figure 24*.

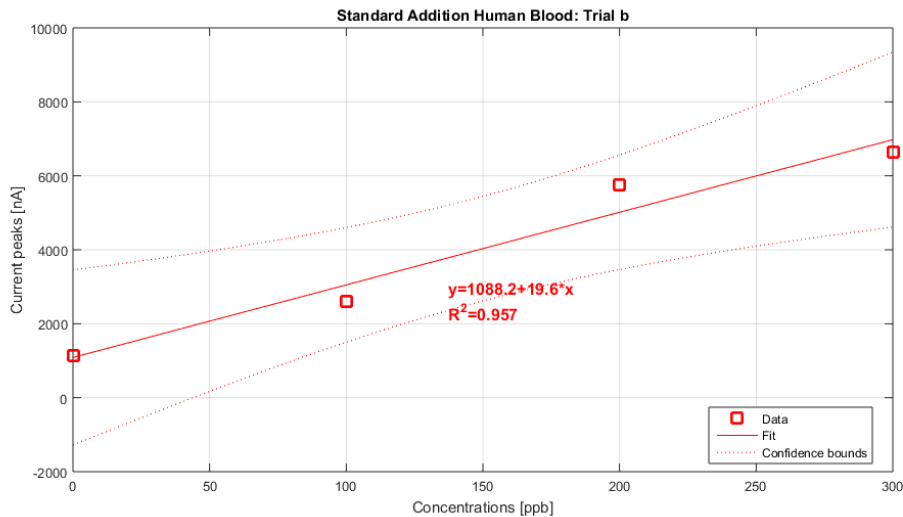


Figure 24-Linear regression model extrapolated from the standard addition on human blood samples. Digestion performed 04/17/2018, second trial

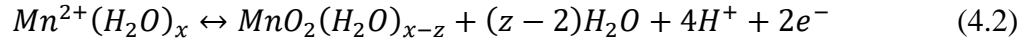
It is important to underline that despite of the non negligible variability in the two estimations, it is possible to assess Pb levels in the range of normal concentrations, well below the established threshold of $180 ppb$. The obtained mean value is therefore $Unknown = 63.1 \pm 12.5 ppb$ with a $CV\% = 19.8\%$, slightly higher than the one obtained in standard solutions at comparable Pb levels ($CV\% = 15\%$). This result turns out to be important, since it ensures that the performances of the sensor are not degraded by the complexity of dealing with biological fluids.

To finally confirm the accuracy of the sensor rather than its precision, comparison with gold standard techniques are on schedule. The same samples of digested blood will be sent to the chemical laboratory at University of Illinois at Urbana-Champaign in order to perform ICP-MS and validate the reliability of the devices, before starting with on the field testing.

4.5. Manganese detection on Pt electrodes

The high electronegativity of Manganese, with a standard reduction potential of $E_0 \cong -1.18V$, makes cathodic stripping voltammetry the most suitable technique for its electrochemical detection.

The reaction that allows Mn detection is the following one^[35]:



During the deposition phase oxidation of Mn to MnO_2 occurs. This involves the imposition of a positive potential for preconcentration and as *Figure 12* points out this prevents Au electrodes from being the proper devices for CSV due to possible interferences with redox reactions involving gold substrate itself (represented by the large anodic and cathodic peaks that appear at positive potentials); among noble metals the most suitable alternative seems to be platinum, even though it is found to be particularly challenging from the first stages of the analysis.

To confirm that Pt substrate provides the proper potential window for Mn detection and to select the best supporting electrolyte a series of cyclic voltammetry is conducted on two different solutions with acetate buffer 0.2M at pH 5.2 and borate buffer 0.1M at pH8.9.

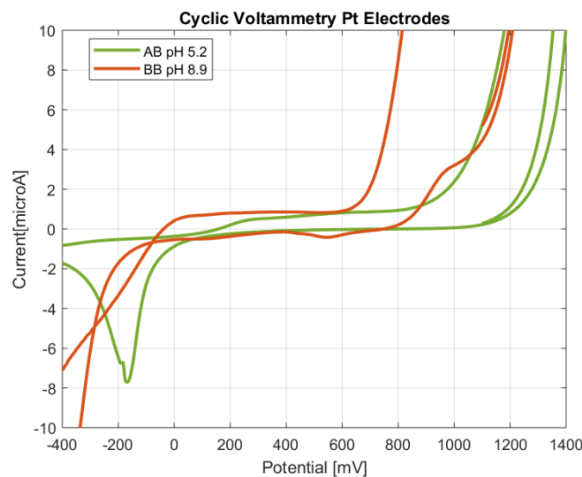


Figure 25 -Cyclic Voltammetry for comparison of the potential window offered by the different supporting electrolytes. Acetate Buffer(AB) pH 5.2 and Borate Buffer (BB) pH8.9 are tested

As shown in *Figure 25* both of the electrolytes provide the proper working window for cathodic stripping voltammetry of Mn. Acetate Buffer guarantees a working window of $\sim 1000\text{mV}$ shifted to more positive potential with respect to the one offered by Borate Buffer and therefore is initially selected as the best supporting electrolyte.

In order to locate the Mn reduction peak an additional series of cyclic voltammetry is conducted in the chosen electrolyte. In contrast with previous works [37], it turns out that no peaks can be easily resolved from the background, despite the high Mn concentrations, as it is possible to grasp from *Figure 26*.

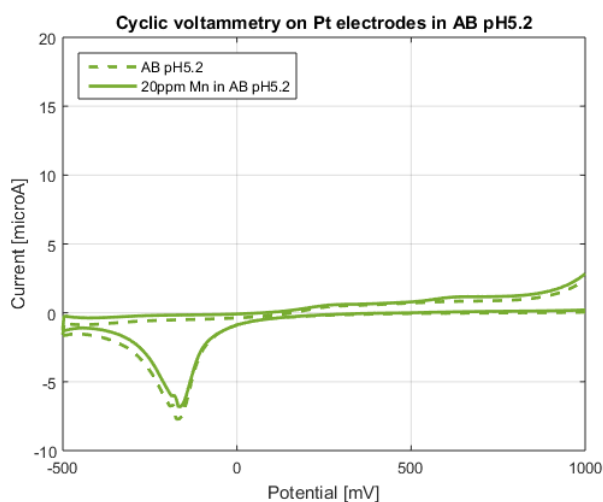


Figure 26-Cyclic Voltammetry of AB pH5.2 alone and with the addition of 20ppm Mn

This absence of signal is initially attributed to a too acidic pH that does not ensure the proper environment for Mn oxidation, but adjusting the pH of the supporting electrolyte from 5.2 up to pH 6.5 with the addition of $\text{NaOH}_{(s)}$ does not improve the detection.

Borate Buffer is therefore taken into consideration as the proper buffer. As depicted in *Figure 27*, a resolved peak can be identified. To confirm that it is related to the Mn reduction a further test with a solution of 40ppm Mn is conducted. The amplitude of the peak increases with

increasing concentrations of the analyte and a slight shift on more positive potentials is evaluated from $E_{red} \sim 500mV$ at 20ppm Mn to $E_{red} \sim 560mV$ at 40ppm Mn.

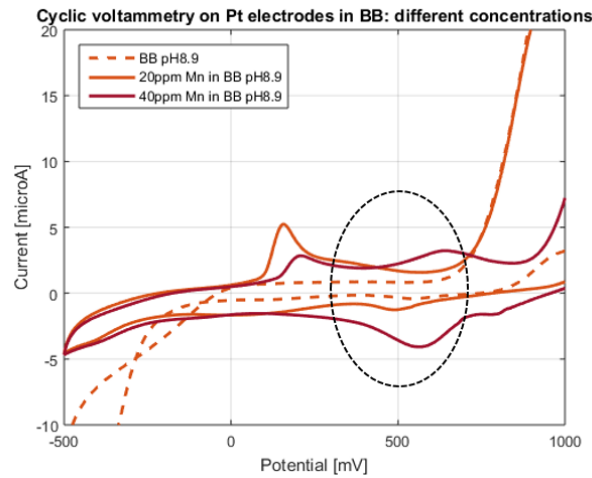


Figure 27-Cyclic Voltammetry of Mn in BB 0.1M pH8.9 at two different concentrations.

4.5.1. Optimization of the SWCSV parameters

As highlighted in the previous section for Pb detection a preliminary optimization of the deposition and stripping phase is required in order to maximize the performances of the sensors. For each parameter triplicate measurements ($n_{rep}=3$) are conducted to achieve a sufficient statistical significance. In order to achieve a well-resolved signal even in non ideal conditions for the analysis 10 μ L sample droplets with a concentration of 100ppb Mn in BB 0.1M at pH 8.9 are tested .

- **Deposition Phase**

The first variable considered for the optimization is the deposition potential, known to have a great impact on the acquired signal. Interestingly a only a deposition potential $E_{dep} = 700mV$ is found to provide a repeatable voltammogram. For potentials $E_{dep} \leq 600mV$ in several cases no signal was acquired, meaning that the potential is not enough positive to favor the oxidation of Mn^{2+} . On the other side, at deposition potentials $E_{dep} \geq 800mV$ significant distortion in the curve occur. Conversely ,at a deposition potential $E_{dep} = 700mV$ a coefficient of variation $CV\% = 4.70\%$ is

obtained even at quite short deposition times $t_{dep} = 450s$ (evaluated on $n_{rep}=5$). The current peak settled at a mean potential $E_{peak} = 472.9mV \pm 7.5mV$ with a mean cathodic peak $i_{peak} = 495nA$.

The second relevant feature to be selected is the deposition time, during which the constant $E_{dep} = 700mV$ is provided to the working electrode. The range $120s-1200s$ is taken into account. As it is enhanced by the graph in *Figure 28* after 900s the mean signal levels off, indicating that all of the Mn in $10\mu L$ droplet is concentrated onto the working electrode.

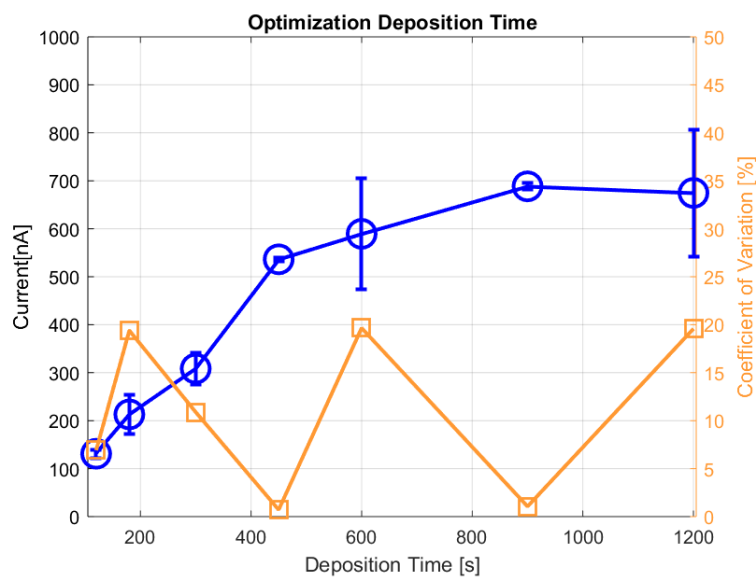


Figure 28-Optimization of the deposition time from 120s to 1200s of Manganese in BB 0.1M pH8.9

At this point the first issues appear; in fact, after several experiments, it turns out that, in order for the sensor to detect lower concentrations of Mn a $t_{dep} = 900s$ is not enough and increasing it up to 1200s significantly improves the signal. The mean values for the peak current on 3 repetitions at 5ppb Mn with $t_{dep} = 900s$ and $t_{dep} = 1200s$ are respectively $i_{900s} = 42.3nA$ and $i_{1200s} = 123.2nA$.

A deposition time $t_{dep} = 1200s$ is therefore selected in order to maximize the performances of the sensor at low Mn concentrations.

The optimized parameters at the end of this process are $E_{dep} = 700mV$ and $t_{dep} = 1200s$.

- **Square Wave**

For the proper tuning of the parameters of the square wave a deposition potential $E_{dep} = 700mV$ and a deposition time $t_{dep} = 450s$ are selected. As emerged from the analysis on Pb detection both the square wave amplitude and the square wave period can have an impact on the magnitude and on the shape of the current peaks.

Square wave period is analyzed from $\tau_{min} = 10ms$ to $\tau_{max} = 100ms$. *Figure 29* underlines the decrease of the peak magnitude with increasing the period of the square wave, in accordance with the theory. Even though the need for repeatability is one of the main feature to be considered, in the case of Mn detection at trace level only the parameters that maximize its value allow a resolution from the background down to $5ppb$ of Mn concentration. Therefore $\tau_{min} = 10ms$ is selected as the optimum square wave period.

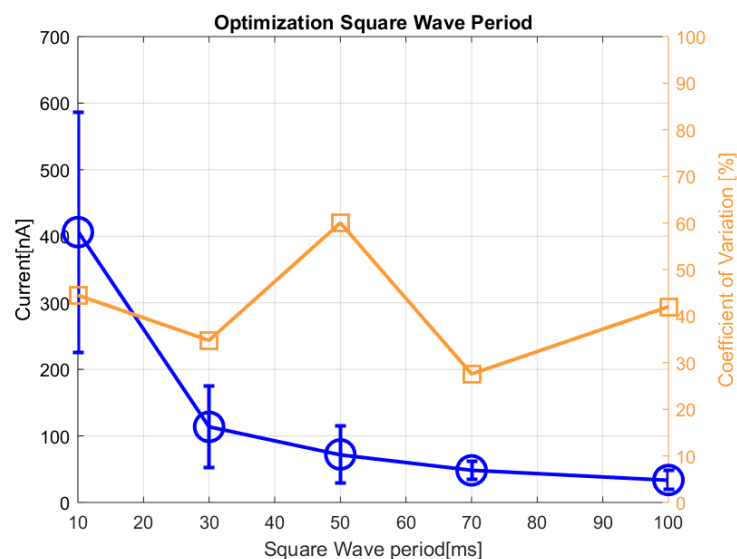


Figure 29-Optimization of the square wave period for Mn detection on Pt electrodes.

As a parallel path with analysis of the parameters for Pb detection square wave amplitude is initially examined in the range $E_{sw} \text{ min} = 17.5\text{mV}$ - $E_{sw} \text{ max} = 100\text{mV}$, but as shown in *Figure 30* the magnitude of the cathodic peak current seems to follow a linear trend as a function of the amplitude of the square wave and therefore an analysis up to $E_{sw} \text{ max} = 150\text{mV}$ is carried out.

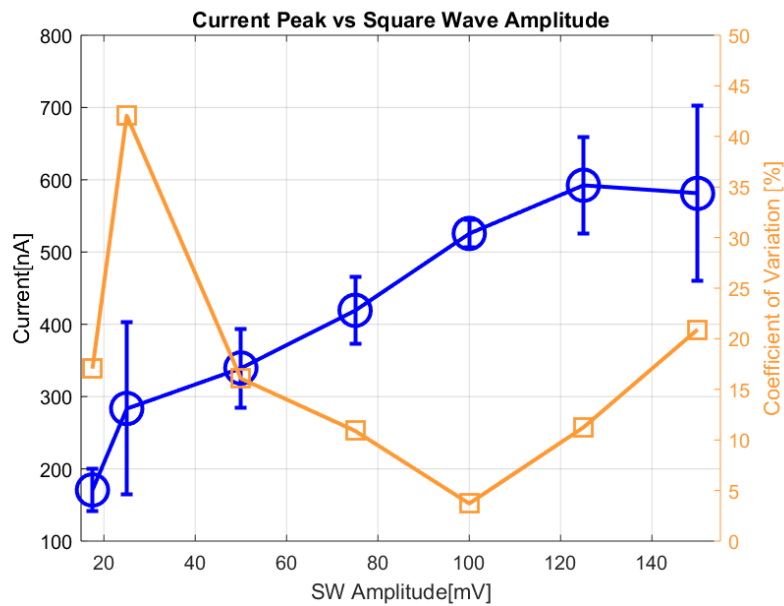


Figure 30-Magnitude of the cathodic peak current of 100ppb Mn in BB as a function of the square wave amplitude and corresponding CV%

As pointed out several times in these pages not only the magnitude of the current peak but also its variability is fundamental for repeatability in practical applications. A square wave amplitude of $E_{sw} = 100\text{mV}$ is therefore selected as the one that guarantees the minimum coefficient of variation $CV\% = 3.71\%$.

The analytical parameters selected for the calibration of the Pt sensor for the detection of Mn in borate buffer solutions are sum up in TABLE VII.

TABLE VI-OPTIMIZED PARAMETERS FOR SWCSV OF Mn ON Pt ELECTRODES.
SUPPORTING ELECTROLYTE:BB pH8.9

PARAMETER	VALUE
DEPOSITION TIME	1200s
DEPOSITION POTENTIAL	0.7V
SQUARE WAVE AMPLITUDE	100mV
SQUARE WAVE PERIOD	10ms
STEP POTENTIAL	5mV

4.6. Calibration

In accordance with the Mn range typically found in human blood – 4.7ppb – 18.3ppb-^[35]the selected range for calibration is 5ppb – 100ppb . The capabilities of the Pt sensor of resolving a Mn concentration down to 5ppb are demonstrated by the plot in *Figure 31*,.Repetitions on three different electrodes provide a mean peak $i_{peak5ppb} = 82.8nA$ and a coefficient of variation $CV\% = 22.8\%$,but further analysis are still required in order to assess a reliable calibration curve.

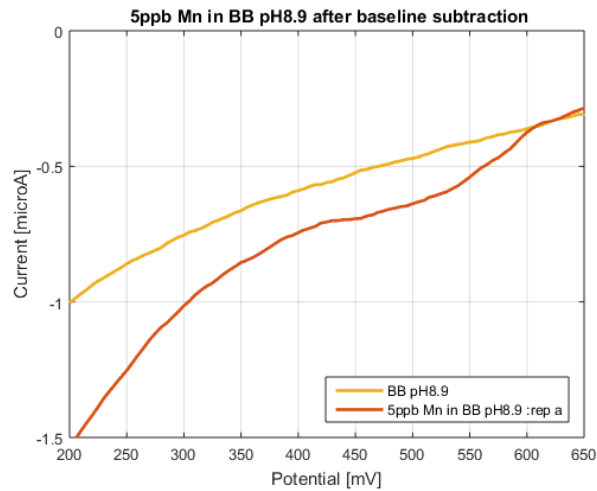


Figure 31- Detection of 5ppb Mn in borate buffer pH8.9 through SWASV on Pt sensors

4.7. Human Blood

In addition, analysis of blood samples introduces two other issues that make Mn detection challenging but interesting at the same time. The first one is the dilution factor required in order to bring the digested sample up to basic pH and the second one is the precipitation of Manganese (II) hydroxide as a consequence of the addition of Sodium Hydroxide ($NaOH$) required for pH adjusting. These obstacles do not prevent the constant research for innovative strategies and successful Mn detection is just delayed.

CHAPTER 5

CONCLUSIONS AND WORK IN PROGRESS

The performances of small and low cost sensors for electrochemical detection of lead (*Pb*) are demonstrated in standard solutions and optimized to achieve full compatibility with human blood testing. Their main advantages over more sensitive but less practical sensors based on carbon nanotubes^[38] or bismuth^[39] include ease of fabrication in large amounts, ability to successfully detect heavy metals at trace levels in reduced droplets of only 10 μ L and the possibility of integration in electrochemical arrays for a complete automatization of the standard addition procedure in the next future.

Gold-based sensors for lead (*Pb*) assessment are able to achieve $LOD = 7.86ppb$ (38nM), far below the value that in human blood requires medical attention -180ppb for the adults and 50ppb for children-^[33]. First tests on human blood samples demonstrated good precision, even though for estimation of their accuracy comparison with well established techniques needs to be performed.

Detection of manganese (*Mn*) turns out to be more challenging, as far as its concentration in human blood ranges in between 4ppb-15ppb. It is proven that Pt sensors are able to detect such low concentrations but repeatability issues are found.

Minor improvements are still needed in order to pursue the dream of E-CHeMA , or metallometers for home-care monitoring of heavy metals, but the right path is traced and electrochemical sensing is mature enough for exiting the academic environment. The two most critical aspects that are worth to be pointed out are the reproducibility of signal, that is affected by a variety of parameters not fully taken into account in this preliminary study and the sample pretreatment. This last passage still requires handling with dangerous chemicals, such as nitric acid (HNO_3) and hydrogen peroxide (H_2O_2) , high and controllable temperatures and human

intervention in pipetting the different reagents. The final goal will be to make it feasible in an automatic microfluidic device to achieve a complete integration with the subsequent electrochemical detection.

The exponential progresses of the technologies related to the microscale world of both fluids (microfluidic) and ion-electron interaction (electrochemistry) are a promising carrier to the presence of E-ChEMA in houses, hospitals and factories in the next future

APPENDIX
ELSEVIER LICENSE
TERMS AND CONDITIONS

Apr 20, 2018

This Agreement between UIC -- Elena Boselli ("You") and Elsevier ("Elsevier") consists of your license details and the terms and conditions provided by Elsevier and Copyright Clearance Center.

License Number	4333270167842
License date	Apr 20, 2018
Licensed Content Publisher	Elsevier
Licensed Content Publication	Biosensors and Bioelectronics
Licensed Content Title	A review on various electrochemical techniques for heavy metal ions detection with different sensing platforms
Licensed Content Author	BabanKumar Bansod,Tejinder Kumar,Ritula Thakur,Shakshi Rana,Inderbir Singh
Licensed Content Date	Aug 15, 2017
Licensed Content Volume	94
Licensed Content Issue	n/a
Licensed Content Pages	13
Start Page	443
End Page	455
Type of Use	reuse in a thesis/dissertation
Portion	figures/tables/illustrations
Number of figures/tables/illustrations	1
Format	electronic
Are you the author of this Elsevier article?	No
Will you be translating?	No
Original figure numbers	Fig. 4. Classification tree for various electrochemical methods for HMI detection
Title of your thesis/dissertation	EChEMA-Electrochemical sensors for heavy metal analysis
Expected completion date	May 2018
Estimated size (number of pages)	50
Requestor Location	UIC Corso Mazzini 76/D Lodi, LO 26900 Italy Attn: UIC

APPENDIX (continued)

Publisher Tax ID	GB 494 6272 12
Total	0.00 USD

CITED LITERATURE

- [1] Berg, K. E., Adkins, J. A., Boyle, S. E., & Henry, C. S. (2016). Manganese Detection Using Stencil-printed Carbon Ink Electrodes on Transparency Film. *Electroanalysis*, 28(4), 679–684. <http://doi.org/10.1002/elan.201500474>
- [2] J. Jin, F. Xu, and T. Miwa, “Cathodic Stripping Voltammetry for Determination of Trace Manganese with Graphite a Styrene-Acrylonitrile Copolymer Composite Electrodes,” pp. 610–615, 2000.
- [3] Z. L. He, X. E. Yang, and P. J. Stoffella, “Trace elements in agroecosystems and impacts on the environment,” vol. 19, pp. 125–140, 2005.
- [4] S. Wang and X. Shi, “Molecular mechanisms of metal toxicity and carcinogenesis,” pp. 3–9, 2001.
- [5] Mayo Clinic website <https://www.mayoclinic.org/diseases-conditions/lead-poisoning/in-depth/lead-exposure/art-20044627> [Online; accessed 03/23/2018]
- [6] H. Needleman, “Lead Poisoning,” *Annu. Rev. Med.*, vol. 55, no. 1, pp. 209–222, 2004.
- [7] P. B. Tchounwou, C. G. Yedjou, A. K. Patlolla, and D. J. Sutton, “Heavy Metals Toxicity and the Environment,” pp. 1–30, 2014.
- [8] W. Laohaudomchok, X. Lin, R. F. Herrick, S. C. Fang, J. M. Cavallari, R. Shrairman, A. Landau, D. C. Christiani, and M. G. Weisskopf, “Neuropsychological effects of low-level manganese exposure in welders,” *Neurotoxicology*, vol. 32, no. 2, pp. 171–179, 2011.
- [9] G. Aragay, J. Pons, and A. Merkoçi, “Recent trends in macro-, micro-, and nanomaterial-based tools and strategies for heavy-metal detection,” *Chem. Rev.*, vol. 111, no. 5, pp. 3433–3458, 2011.
- [10] T. Alizadeh and S. Amjadi, “Preparation of nano-sized Pb²⁺ imprinted polymer and its application as the chemical interface of an electrochemical sensor for toxic lead determination in different real samples,” *J. Hazard. Mater.*, vol. 190, no. 1–3, pp. 451–459, 2011.
- [11] B. L. Gulson, K. J. Mizon, M. J. Korsch, D. Howarth, A. Phillips, and J. Hall, “Impact on blood lead in children and adults following relocation from their source of exposure and contribution of skeletal tissue to blood lead,” *Bull. Environ. Contam. Toxicol.*, vol. 56, no. 4, pp. 543–550, 1996.
- [12] F. Barbosa, J. E. Tanus-Santos, R. F. Gerlach, and P. J. Parsons, “A Critical Review of Biomarkers Used for Monitoring Human Exposure to Lead: Advantages, Limitations, and Future Needs,” *Environ. Health Perspect.*, vol. 113, no. 12, pp. 1669–1674, 2005.
- [13] Aaron B. Bowman, Gunnar F. Kwakye, Elena Herrero Hernández, Michael Aschner, “Role of manganese in neurodegenerative diseases”, *J Trace Elem Med Biol.* 2011 December ; 25(4): 191–203. doi:10.1016/j.jtemb.2011.08.144.
- [14] B. S. Levy and W. J. Nassetta, “Neurologic effects of manganese in humans: A review,” *Int. J. Occup. Environ. Health*, vol. 9, no. 2, pp. 153–163, 2003.

CITED LITERATURE (continued)

- [15] M. Aschner and J. L. Aschner, "Manganese neurotoxicity: Cellular effects and blood-brain barrier transport," *Neurosci. Biobehav. Rev.*, vol. 15, no. 3, pp. 333–340, 1991.
- [16] Bowman, Aaron B. et al. "Role of Manganese in Neurodegenerative Diseases." *Journal of trace elements in medicine and biology: organ of the Society for Minerals and Trace Elements (GMS)* 25.4 (2011): 191–203. *PMC*. Web. 19 Apr. 2018.
- [17] R. Thomas, *Practical Guide to ICP-MS*, Marcel Dekker Inc., vol. 53. 2004.
- [18] A. J. Bard and L. R. Faulkner, *Fundamentals and Fundamentals and Applications*, vol. 8, no.c. 2015.
- [19] Yantasee, W., Lin, Y., Hongsirikarn, K., Fryxell, G.E., Addleman, R., Timchalk, C. "Electrochemical sensors for the detection of lead and other toxic heavy metals: the next generation of personal exposure biomonitoring." (2007) *Environmental health perspectives*, 115 (12), pp. 1683-1690. Cited 86 times. DOI: 10.1289/ehp.10190
- [20] Wang, J. (2005), "Stripping Analysis at Bismuth Electrodes: A Review." *Electroanalysis*, 17: 1341-1346. doi:[10.1002/elan.200403270](https://doi.org/10.1002/elan.200403270)
- [21] Grégoire Herzog, Valerio Beni, "Stripping voltammetry at micro-interface arrays: A review", *Analytica Chimica Acta*, Volume 769, 2013, Pages 10-21, ISSN 0003-2670, <https://doi.org/10.1016/j.aca.2012.12.031>.
- [22] P.T.Kissinger, W.R.Heineman, *Fundamental Concepts of Analytical Electrochemistry in Laboratory Techniques in Electroanalytical Chemistry*, pages 141-143, Marcel Dekker, NY, 2nd ed., 1996.
- [23] B. K. Bansod, T. Kumar, R. Thakur, S. Rana, and I. Singh, "A review on various electrochemical techniques for heavy metal ions detection with different sensing platforms," *Biosens. Bioelectron.*, vol. 94, no. January, pp. 443–455, 2017.
- [24] P.T.Kissinger, W.R.Heineman, J.Wang, *Fundamental Concepts of Analytical Electrochemistry in Laboratory Techniques in Electroanalytical Chemistry*, pages 719-731, Marcel Dekker, NY, 2nd ed., 1996.
- [25] J. G. Osteryoung and R. A. Osteryoung, "Square Wave Voltammetry," *Anal. Chem.*, vol. 57, no. 1, pp. 101–110, 1985. DOI: 10.1021/ac00279a004
- [26] W. Kang, C. Rusinek, A. Bange, E. Haynes, W. R. Heineman, and I. Papautsky, "Determination of Manganese by Cathodic Stripping Voltammetry on a Microfabricated Platinum Thin-film Electrode," *Electroanalysis*, vol. 29, no. 3, pp. 686–695, 2017.
- [27] J. Wang, T. Nakazato, K. Sakanishi, O. Yamada, H. Tao, and I. Saito, "Microwave digestion with HNO₃/H₂O₂ mixture at high temperatures for determination of trace elements in coal by ICP-OES and ICP-MS," *Anal. Chim. Acta*, vol. 514, no. 1, pp. 115–124, 2004.

CITED LITERATURE (continued)

- [28] C. A. Rusinek *et al.*, “Determination of Manganese in Whole Blood by Cathodic Stripping Voltammetry with Indium Tin Oxide,” *Electroanalysis*, pp. 1850–1853, 2017.
- [29] Ellison, Stephen & Thompson, Michael. (2008). “Standard additions: Myth and reality.” *The Analyst*. 133. 992-7. DOI: 10.1039/b717660k
- [30] W. Kang, X. Pei, C. A. Rusinek, A. Bange, E. N. Haynes, W. R. Heineman, and I. Papautsky, “Determination of Lead with a Copper-Based Electrochemical Sensor,” *Anal. Chem.*, vol. 89, no. 6, pp. 3345–3352, 2017.
- [31] S. P. Kounaves, J. J. O’Dea, P. Chandrasekhar, and J. Osteryoung, “Square wave anodic stripping voltammetry at the mercury film electrode: theoretical treatment,” *Anal. Chem.*, vol. 59, no. 3, pp. 386–389, 1987.
- [32] G. Herzog and D. W. M. Arrigan, “Determination of trace metals by underpotential deposition-stripping voltammetry at solid electrodes,” *TrAC - Trends Anal. Chem.*, vol. 24, no. 3 SPEC. ISS., pp. 208–217, 2005.
- [33] Centers for Disease Control and Prevention (CDC) website <https://www.cdc.gov/nceh/lead/> [Online; accessed 03/10/2018]
- [34] C. A. Rusinek, A. Bange, M. Warren, W. Kang, K. Nahan, I. Papautsky, and W. R. Heineman, “Bare and Polymer-Coated Indium Tin Oxide as Working Electrodes for Manganese Cathodic Stripping Voltammetry,” *Anal. Chem.*, vol. 88, no. 8, pp. 4221–4228, 2016.
- [35] Mayo Medical laboratories website <https://www.mayomedicallaboratories.com/test-catalog/Clinical+and+Interpretive/89120>[Online; accessed 02/18/2018]
- [36] C. A. Rusinek, “New Avenues in Electrochemical Systems and Analysis by,” no. August, 2012.
- [37] W. Kang, “point-of-care sensors for determination of manganese in clinical applications.” July, 2016.
- [38] A. Science and w. Kang, “point-of-care sensors for determination of manganese in clinical applications.” *Electroanalysis*, vol. 29, no. 10, 2017.
- [39] Cui, Lin, Jie Wu, and Huangxian Ju. 2015. “Electrochemical Sensing of Heavy Metal Ions with Inorganic, Organic and Bio-Materials.” *Biosensors and Bioelectronics*. Elsevier Ltd. doi:10.1016/j.bios.2014.07.

VITA

NAME Elena Boselli

EDUCATION B.S., Biomedical Engineering, Politecnico di Milano, Milan, Italy, 2016
M.S., Biomedical Engineering, University of Illinois at Chicago, expected May 2018
M.S., Biomedical Engineering, Politecnico di Milano, expected February 2019

WORK Research Assistant at the University of Illinois at Chicago,
January 2018- May 2018

